

Polymetallic Pb-Zn-Ag-In Toyoha Deposit: Geology, Style, Genesis and Exploration

Yasushi Watanabe and Eijun Ohta

Institute for Geo-Resources and Environment, AIST

- 1) Introduction
- 2) Exploration & exploitation history
- 3) Tectonic setting
- 4) Regional geology & metallogeny
- 5) Local geology and geophysics
- 6) Hydrothermal alteration
- 7) Temporal relationship
- 8) Vein system
- 9) Ore-forming stages
- 10) Ore solution chemistry
- 11) Hydrothermal environments and fluid origin
- 12) Synthesis
- 13) Exploration implications
- 14) Exploration technique

References

Copyright 2005 by the Institute for Geo-Resources and Environment, All rights reserved.
Higashi 1-1-1, Tsukuba 305-8567, Japan

Printed in Japan by Asahi Printing Co. Ltd., Tsuchiura

1) Introduction

A link between intermediate, calc-alkaline volcanism and hydrothermal mineralization has been well recognized in the subduction-related magmatic arcs. This link is reflected in the volcanic regions coincident with epithermal metallogenic provinces (John, 2001), stratovolcanoes associated with porphyry Cu deposits as well as base- and precious metal deposits (Sillitoe, 1973, 1977; Lexa et al., 1999), present-day metallic mineralization occurring within the central craters of active volcanoes such as Osorezan (Aoki, 1991), etc. Thus, we have regarded that calc-alkaline, andesitic stratovolcanoes are one of the important exploration objectives for epithermal and porphyry Cu deposits (Sillitoe and Bonham, 1984; Sillitoe, 1995; White et al., 1995; Hedenquist et al., 1996; Fig. 1-1).

However, through mineral exploration programs, we have realized that not all the stratovolcanoes are mineralized; rather, volcanoes associated with significant metallic mineralization are rare in number, and the time span for metallic mineralization is limited in a period of long-lasting volcanic activities in the volcanic fields (Cunningham et al., 1994; Watanabe, 2002). Moreover, base-metal and precious metal deposits tend to form in the different hydrothermal environments in a magmatic-hydrothermal system (Fig. 1-1; Hedenquist et al., 1996). The biggest challenge in mineral exploration in such volcanic fields is, therefore, to differentiate mineralized magmatic-hydrothermal systems from barren ones, and predict the locations of ore deposits and types of the deposits.

The Toyoha polymetallic Pb-Zn-Ag-In deposit, a vein-type epithermal-xenothermal deposit in the Northeast Japan arc, constitutes a part of a mineralized magmatic-hydrothermal system related to the activity of a calc-alkaline andesitic volcano (Muine volcano; Fig. 1-2). This magmatic-hydrothermal system is young in age (Pliocene-Pleistocene) and has been only slightly eroded, resulting in the preservation of surface expression of the hydrothermal alteration. This magmatic-hydrothermal system has been studied from various viewpoints (Table 1-1), which enable us to establish a comprehensive genetic model. The purpose of this paper is to provide essential exploration implications in young calc-alkaline volcanic fields, by introducing a genetic model of the Toyoha deposit.



Fig. 1-2 A view of Mt. Muine. Gray-colored parts beneath the snow are the scarps formed by landsliding.

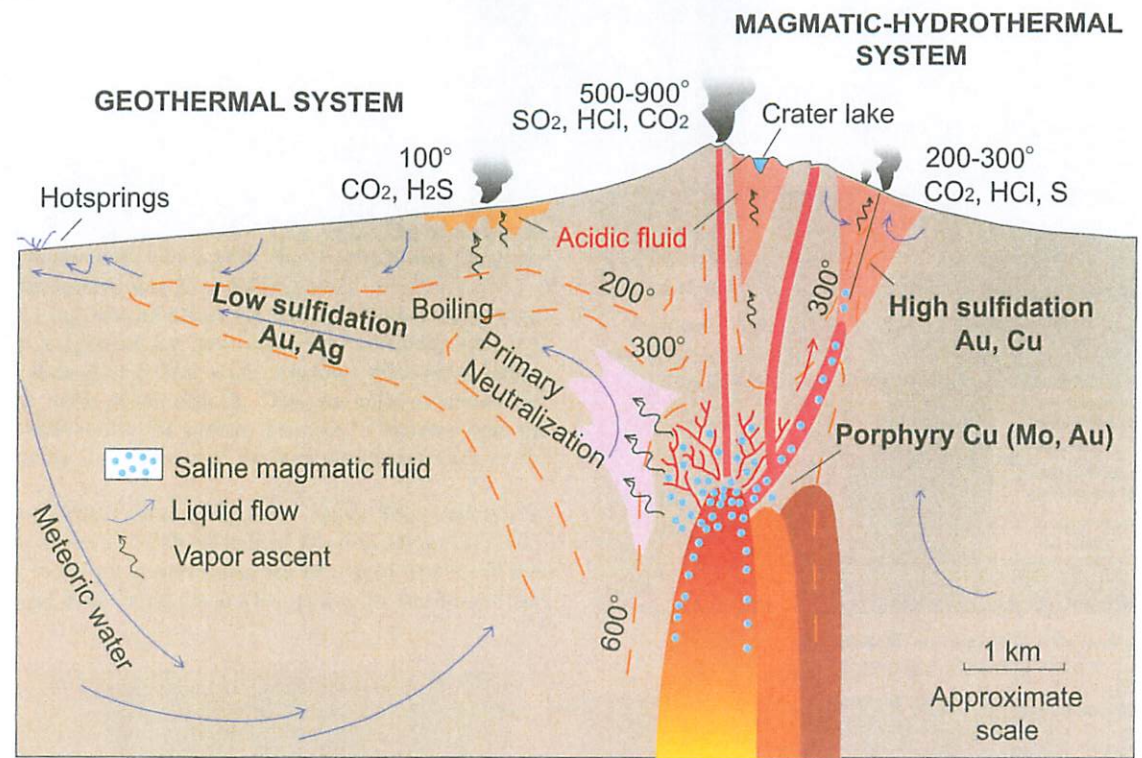


Fig. 1-1 Schematic figure of a magmatic-hydrothermal system showing the relationship among a stratovolcano, hydrothermal deposits and hydrothermal alteration (Hedenquist et al., 1996).

Table 1-1 Major studies related to the Toyoha polymetallic deposit

Topic	Sub-topic	References
Tectonics	Tectonic history	Watanabe (2002)
Geology	Regional geology	Watanabe & Iwata (1986), Watanabe (1990a)
	Local geology	Miyajima et al. (1971), Kuwahara et al. (1983)
Structure	Regional structures	Watanabe (1989)
	Vein structure	Akome & Haraguchi (1967), Watanabe (1990b), Watanabe & Ohta (1995)
Geochronology		Sawai et al. (1989)
Mineralization		Ohta (1989, 1991, 1992)
Alteration		Sawai (1984)
Stable isotopes	Oxygen	Matsuhisa et al. (1986)
	Sulfur	Hamada and Imai (2000), Watanabe (2003a)
Fluid inclusions		Yajima & Ohta (1979), Ono & Sato (1994), Shimizu & Aoki (2001a)
Geophysics	MT	Takakura & Matsushima (2003)
Geothermics	30m-depth temperature	NEDO (1988)
Exploration	GEOGAS method	Metal Mining Agency of Japan (1991)

2) Exploration & exploitation history

The Toyoha deposit is located about 30 km west-southwest of the city center of Sapporo in the Sapporo-Iwanai district in Hokkaido, Japan. The district is situated at the junction between the north-trending Northeast Japan arc and east-northeast-trending Kuril arc (Fig. 2-1). Although the discovery age of the deposit is unknown, the first reports of the deposit were published in the late 19th century. These reports describe the presence of abandoned adits along the Shirai River, a stream running parallel to the major veins of the deposit. The Kuhara Mining, which was succeeded presently by the Nippon Mining & Metals Co., acquired the deposit in 1914 and exploited silver ore near the surface until 1922. The deposit was reopened in 1935 and exploited lead, zinc and silver, but was closed in 1944 due to collapsing in the mine. Since 1950, the Toyoha Mines Co. Ltd., one of the satellite mining companies of the Nippon Mining & Metals Co., has been exploiting the deposit over 55 years (Fig. 2-2).

In order to expand the ore reserves of the deposit, the Metal Mining Agency of Japan and the Toyoha Mines Co. Ltd. performed three-stage diamond drilling programs during the periods of 1973-1977, 1988-1992 and 1993-1995 with support of the government of Hokkaido. The first program detected some manganese-rich ore veins on the northwest of the deposit, and the second and third stage programs discovered major polymetallic veins (e.g. Shinano) rich in silver and copper in addition to zinc and lead on the south of the deposit. Thus, the mine extended the deposit towards the south (Fig. 2-3) and started copper production from 1991. These newly discovered veins contain a couple of hundred ppm of indium, and since 1980, indium has been recovered from the zinc concentrate as byproduct, leading Japan as one of the largest indium producers in the world (Figs. 2-4 and 2-5).

The deposit has produced more than 20 Mt of ore in total, including 1.8 Mt zinc, 0.49 Mt lead, 3000 t silver, and 8,000 t copper. The monthly ore production in 2003 was 32,400 t at the grades of 310 g/t silver, 2.1 % lead, 11.2 % zinc, 0.6 % copper and 310 g/t indium (Toyoha Mines Co. Ltd., unpublished data). Compared with the silver grade, gold grade of the ore is extremely low; 0.3 to 0.4 g/t, nevertheless, the total gold amount of the deposit exceeds 10 t (Kanbara and Kumita, 1990). Copper, lead and zinc concentrates are produced in the mine site and shipped to the smelters of the Nippon Mining & Metals Co. through Otaru City.

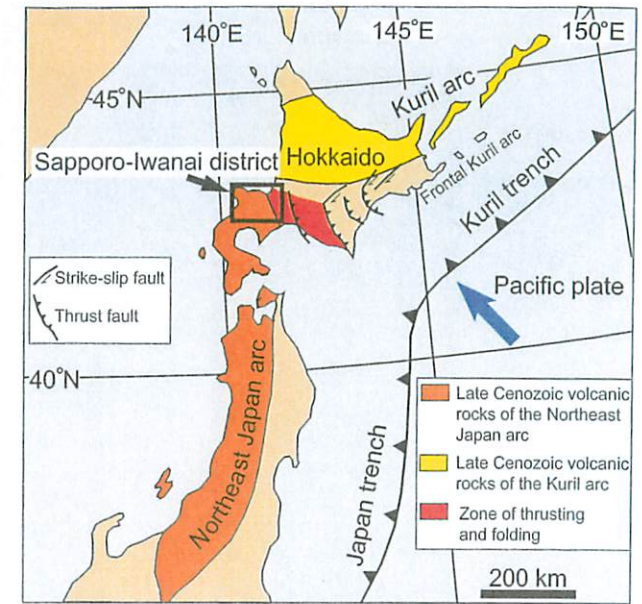


Fig. 2-1 Present tectonic setting of Northern Japan and the location of the Sapporo-Iwanai district.



Fig. 2-2 Toyoha mine.

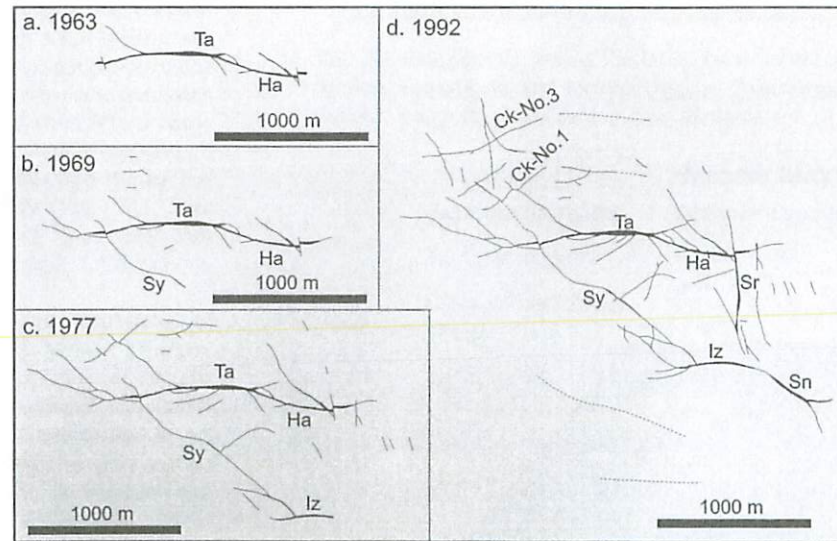


Fig. 2-3 Plan views of the vein systems of the Toyoha mine in 1963 (a), 1969 (b), 1977 (c) and 1992 (d) (Yajima et al., 1993). Abbreviation of the vein names is; Ck: Chikugo, Ha: Harima, Iz: Izumo, Ta: Tajima, Sn: Shinano, Sr: Sorachi, and Sy: Soya.



Fig. 2-4 Ingot of indium.

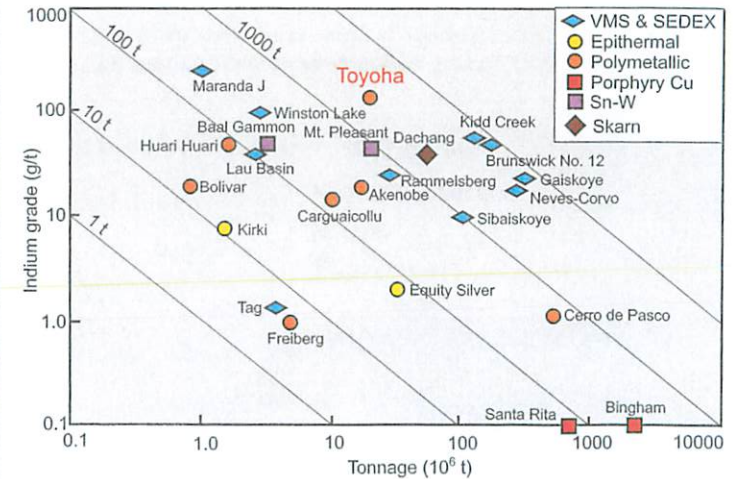


Fig. 2-5 Indium grade versus tonnage relationships for representative indium-bearing deposits (Schwarz-Schampera and Herzig, 2002).

3) Tectonic setting

The Sapporo-Iwanai district in southwest Hokkaido, where the Toyoha deposit is included, is underlain by a Jurassic accretionary complex of the Eurasian continental margin, upon which a magmatic arc was built during the Cretaceous and Paleogene. Early Miocene backarc spreading separated the arc from the Eurasian continent, and since then, the district has been located at the northern end of the Northeast Japan arc.

Since the Middle Miocene, the tectonic regime of southwest Hokkaido has been related to the orthogonal convergence rate (OCR) between the Northeast Japan arc and the Pacific plate, and the collision of the frontal Kuril arc with the Northeast Japan arc. Due to the fluctuation of the subduction direction of the Pacific plate, the OCR changed from the Middle Miocene low OCR (5-8 cm/y) to the Pliocene-Early Pleistocene high OCR (9-10 cm/y) through the Late Miocene intermediate OCR (7-9 cm/y) (Watanabe, 2002). The Middle and Late Pleistocene period is characterized by decreasing OCR from 9 cm/y to 6 cm/y due to rapid clockwise rotation of the Pacific plate (Watanabe, 2002; Fig. 3-1).

The Middle Miocene low OCR period is characterized by tholeiitic andesitic volcanism in the volcanic front region and bimodal volcanism of basalt and rhyolite in the backarc region. The Late Miocene intermediate OCR period and the Pliocene-Early Pleistocene high OCR period are dominant in calc-alkaline andesitic volcanism, with minor dacitic activities in the volcanic front region. Tholeiitic andesite again has become dominant since the Middle Pleistocene when the OCR decreased from 9 to 6 cm/y. The location of the volcanic front fluctuated, corresponding to the change of the OCR; the front shifted trenchward and backarc-ward during the periods of relatively low and high OCR, respectively (Fig. 3-1). This suggests the change of the dip of the subduction slab from steep slab during the low OCR periods to gentle slab during the high OCR periods (Fig. 3-2).

Tectonic regimes and regional stress fields, inferred from styles of faulting, folding and dike orientation, changed from Middle Miocene extensional regime with arc-normal minimum compressional stress (σ_3) to Pliocene-Early Pleistocene neutral regime with arc-normal maximum compressional stress (σ_1). The Late Miocene regime, characterized by no major faulting and folding and radial pattern of dikes in polygenetic volcanoes, may have been intermediate between the Middle Miocene and Pliocene-Early Pleistocene regimes with small differential stress (Watanabe, 2002; Fig. 3-1).

Fig. 3-2 Schematic figures showing the relationships among the tectonic regime, stress field, style of volcanism and subduction mode (Watanabe, 2002).

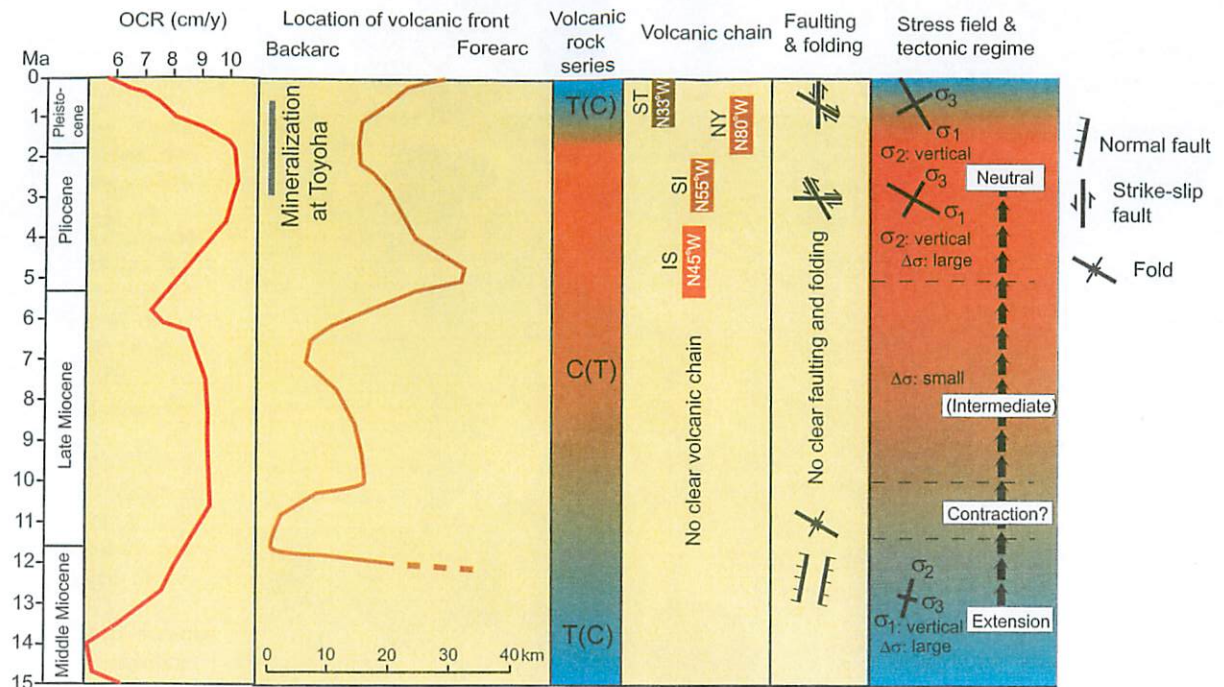
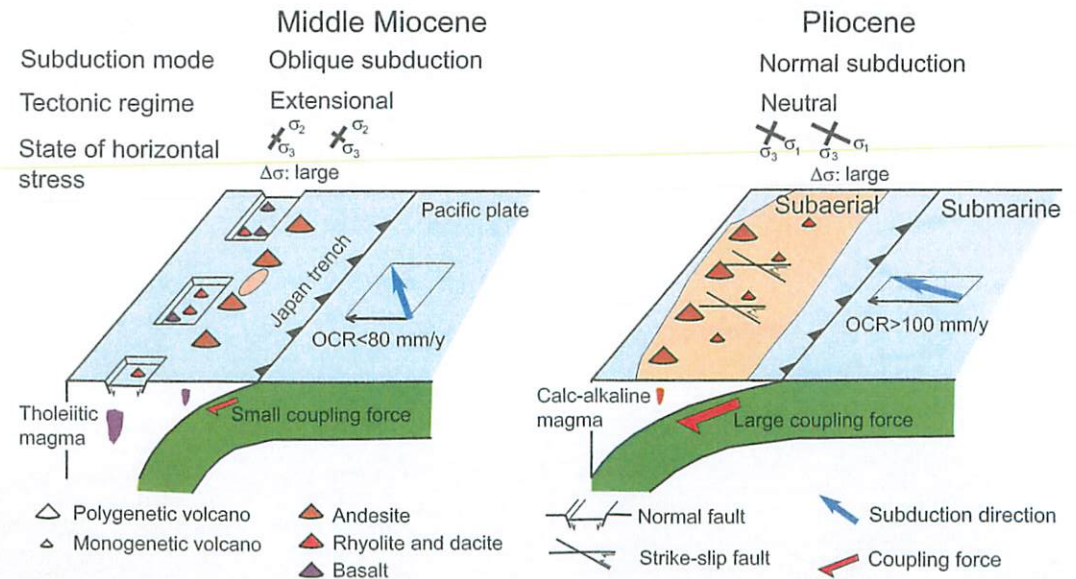


Fig. 3-1 Relationship among the OCR, location of volcanic front, volcanic rock series, trend of volcanic chain, faulting and folding, stress field and tectonic regime (Watanabe, 2002). C(T): calc-alkaline series dominant (minor tholeiitic), T(C): tholeiite series dominant (minor calc-alkaline).



4) Regional geology & metallogeny

The Sapporo-Iwanai district has a thick cover of Miocene volcanic rocks overlying Mesozoic sedimentary and volcanic rocks. The Early and Middle Miocene formations consist of shallow marine sedimentary and volcanic rocks. The Late Miocene formations consist of andesitic hyaloclastites, interfingering with shallow marine sedimentary rocks and subaerial massive andesite lavas.

The Pliocene and Pleistocene units consist mainly of subaerial volcanic rocks that formed polygenetic volcanoes. In particular, some of the Late Pliocene and Early Pleistocene volcanoes, such as Muine and Niseko, form composite volcanoes consisting of multiple polygenetic volcanoes. The Pliocene and Pleistocene volcanoes form northwest-striking volcanic chains, concordant with the assumed subduction directions of the Pacific plate; N45°W Ishikura-Shimamatsu (IS) chain, N55°W Shakotan-Izari (SI) chain, N80°W Niseko-Yotei (NY) chain and N33°W Sapporo-Tarumai (ST) chain (Watanabe, 1993; Fig. 4-1). During the latest Pleistocene, the Shikotsu volcano erupted a huge volume of rhyolitic ash-flow and fall deposits that cover the eastern margin of the district, forming a caldera lake in the southeast of the district (Fig. 4-2a).

The late Cenozoic strata are generally subhorizontal and there is no major structural zone in the district, although the district includes many minor faults and shear zones. These faults include the Middle Miocene north-northeast-striking normal faults and Pliocene east-striking right-lateral and northwest-striking left-lateral strike-slip faults. The Middle Miocene and Pliocene faults are located mainly in the backarc and volcanic front regions of the district, respectively. Displacements along these faults are commonly less than a couple of hundred meters.

The district includes Kuroko and vein-type epithermal deposits (Figs. 4-2a and b). The Middle Miocene period is characterized by Kuroko mineralization (e. g. Yoichi Cu-Pb-Zn) associated with submarine rhyolitic volcanism in the backarc region. The Late Miocene period lacks major economic deposits, despite of dominance of base-metal vein occurrences, associated with felsic porphyry intrusions and andesitic polygenetic volcanoes (Fig. 4-2b). The Pliocene and Early Pleistocene polygenetic andesite volcanoes are associated commonly with major base-metal or precious metal deposits. These are Toyoha epithermal-xenothermal Pb-Zn-Ag-In, Inakuraishi and Ohe epithermal Mn-Zn-Pb (1.6 Mt Mn, 90,000 t Zn), Chitose LS epithermal Au-Ag (18 t Au), Teine HS epithermal Au-Cu (9 t Au), Todoroki LS epithermal Au-Ag (5.7 t Au) and Koryu LS epithermal Au-Ag deposits (no available production record).

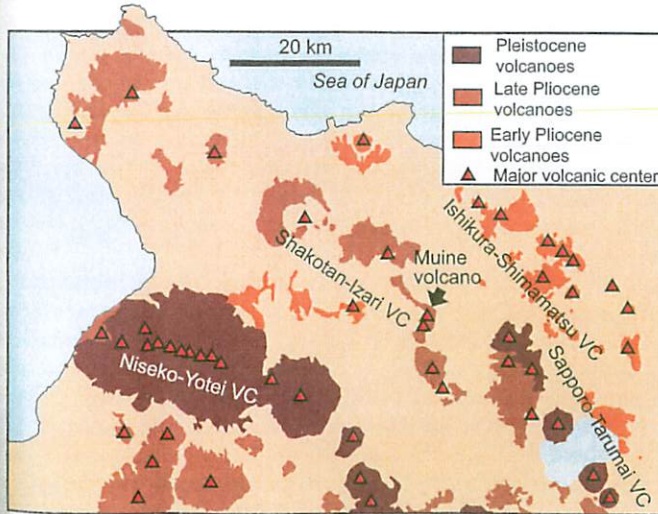


Fig. 4-1 Pliocene-Quaternary volcanic chains (VC) in the Sapporo-Iwanai district. The age ranges of the volcanoes consisting of these chains are; Ishikura-Shimamatsu (5.5-3.7 Ma), Shakotan-Izari (3.3-2.0 Ma), Niseko-Yotei (2.0-0 Ma), and Sapporo-Tarumai (1.2-0 Ma) (Watanabe, 1993).

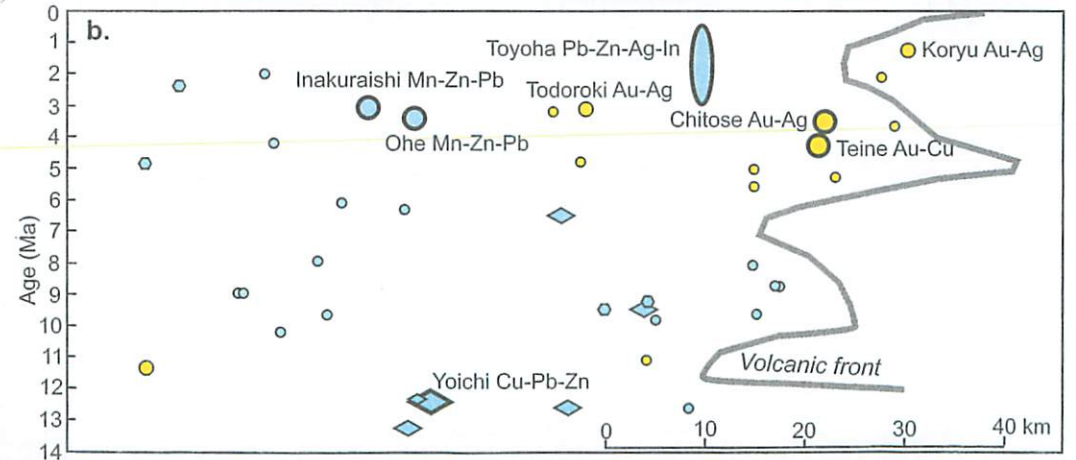
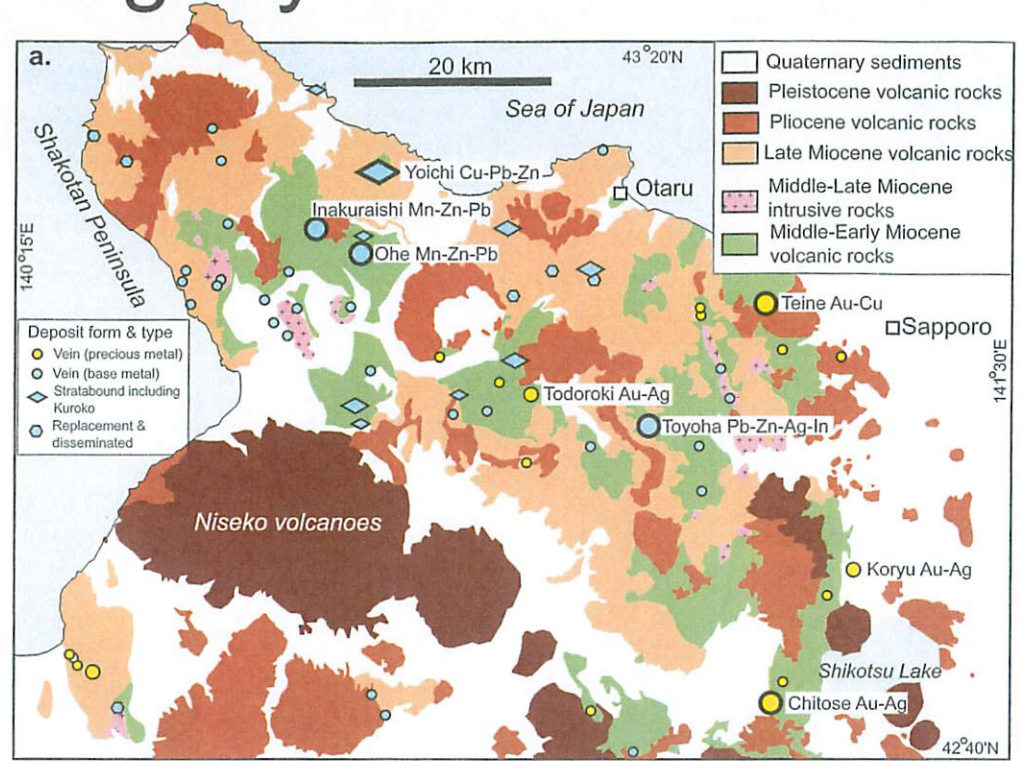


Fig. 4-2 a: Geologic map and distribution of metallic mineral deposits and occurrences of the Sapporo-Iwanai district (Watanabe, 2002). **b:** Age versus longitudinal location of the metallic mineral deposits and occurrences in the Sapporo-Iwanai district (Watanabe, 2002). Location of the volcanic front is also shown.

5) Local geology and geophysics

The pre-Miocene basement in the Toyoha area is a flysch sequence (Usubetsu Formation), which consists of alternating beds of sandstone and mudstone. Granodiorite stocks of Late Oligocene and Miocene age intruded the basement rocks, resulting in biotite hornfels metamorphism. The rocks of this formation are impermeable as compared with those of the Miocene formations. This is represented by the low porosity (1.3 %) of the rocks of this formation than those of the Miocene volcanic (4.4 %) and sedimentary rocks (15.6 %).

An Early and Middle Miocene sequence, 1,000-1,500 m thick around the Toyoha deposit, was deposited in a submarine environment. This sequence consists of the lower volcanic rock-dominant Shiramizugawa Formation and the upper sedimentary rock-dominant Shiraigawa Formation. The andesitic sequence that overlies the Early and Middle Miocene sequence is divided into early Late Miocene hyaloclastites, late Late Miocene subaerial lavas and the Pliocene subaerial lavas that form the Muine, Yoichidake and Kimobetsudake volcanoes (Fig. 5-1). These Late Miocene and Pliocene andesites contain orthopyroxene, clinopyroxene and plagioclase as phenocrysts, and are medium-K, calc-alkaline in composition (Figs. 5-2a and b). The andesites become enriched in SiO₂ from Late Miocene to Pliocene. They have limited ranges of Sr isotopic values (0.7033-0.7048) and Nd isotopic values (0.5126-0.5130), which follow the trend of "the mantle array" (Fujibayashi et al., 1995).

The Pliocene Muine volcano has a N-S elongated volcanic body with a flat ridge (Fig. 1-1 and 5-1), composed of multiple polygenetic volcanoes. Several phreatic craters (Fig. 5-3a), 250-400 m in diameter, occur in the landslide deposits and andesite lavas in the volcano. These craters cluster mainly in two areas (the northern and southern centers). Lacustrine breccia, sandstone and siltstone composed of volcanic fragments (Fig. 5-3b) are observed in these craters. Present-day geothermal activity is not recognized in these craters. Landslide and debris flow deposits (Fig. 5-3c) originated mainly in the northern and southern centers of the phreatic craters. Several arsenic (Fig. 5-3d) and sedimentary monite occurrences present at the margin of the Muine andesite lavas.

Magnetotelluric survey detected an extremely conductive zone beneath the Muine volcano, in addition to a conductive zone near the surface (Fig. 5-4). The surface conductive zone corresponds to the zone of hydrothermal alteration, and the deep conductive zone, of which top is approximately 2 km deep, is interpreted as a large hydrothermal reservoir with abundant hot water or melted magma (Takakura & Matsushima, 2003), because the zone corresponds to an elastic wave attenuation zone detected by a seismic survey (Ohminato & Takakura, 1999).

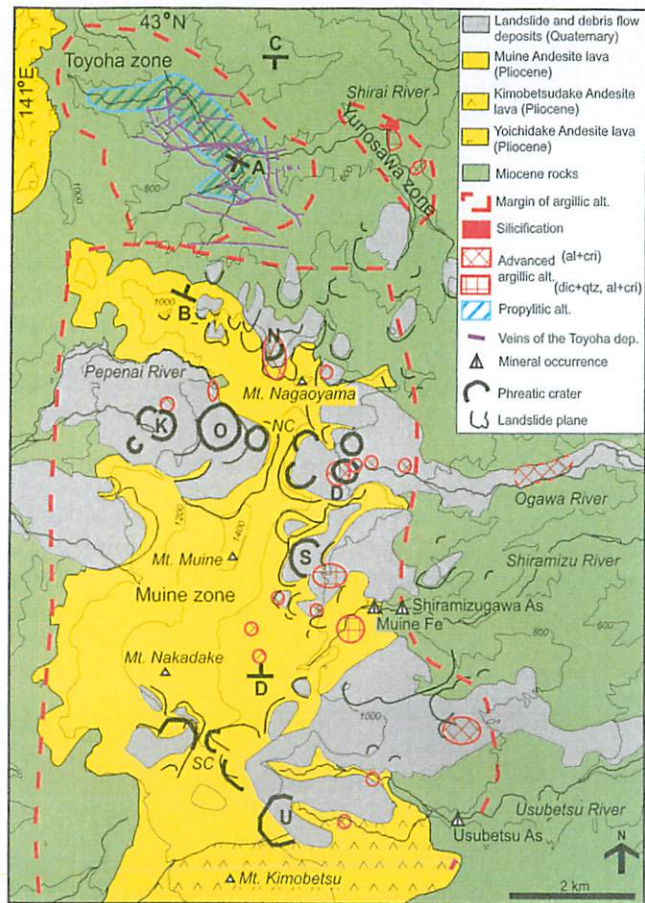


Fig. 5-1 Geologic map and hydrothermal alteration zones of the Toyoha area. Abbreviations of the phreatic craters and crater centers are; D: Daijagahara, K: Konuma, O: Ohnuma, S: Shiramizugawa and U: Usubetsu, NC: northern center, and SC: southern center.

Fig. 5-4 2D resistivity models for the east-west profile of the Toyoha area by the magnetotelluric survey (Takakura and Matsushima, 2003). V.E.: vertical exaggeration.

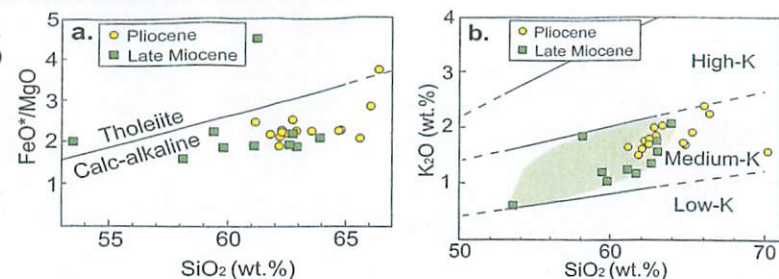


Fig. 5-2 Bulk chemical compositions of the volcanic rocks in the Toyoha area. **a:** SiO₂ versus FeO*/MgO diagram. * Total iron as FeO. **b:** SiO₂ versus K₂O diagram.

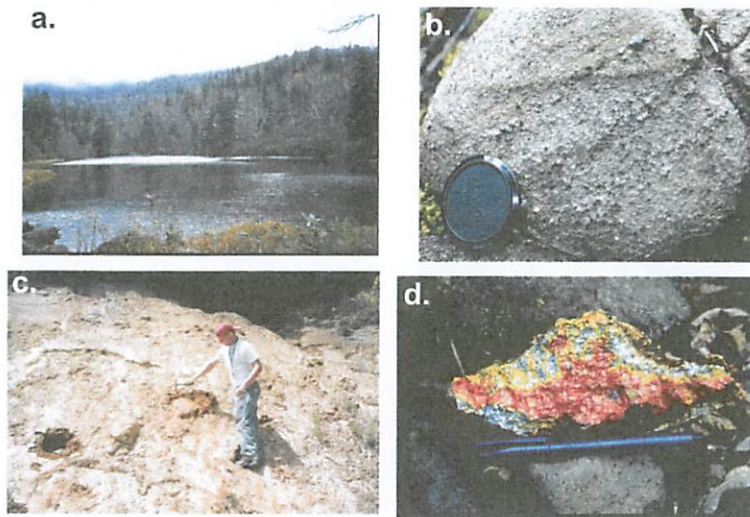
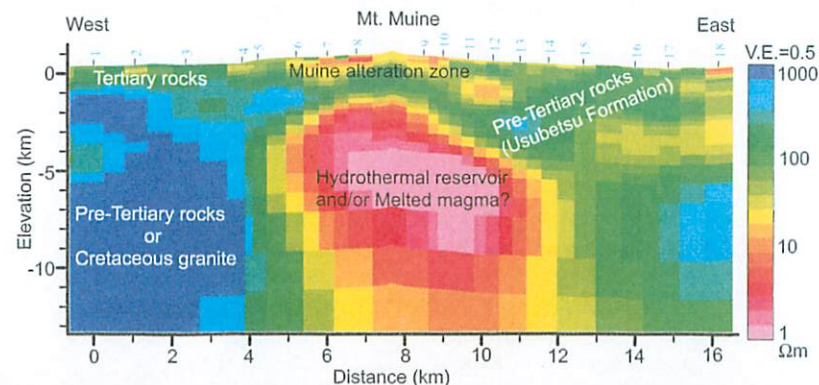


Fig. 5-3 Photographs of a phreatic crater and rocks around the Muine volcano. **a:** phreatic crater at Konuma, **b:** granule-size conglomerate in the Konuma crater, **c:** debris flow deposits along Ogawa river, **d:** arsenic minerals (red: realger, yellow: orpiment) at the Usubetsu occurrence.



6) Hydrothermal alteration

Three major hydrothermal alteration zones of Pliocene-Pleistocene age; Muine, Toyoha and Yunosawa, are developed in the Toyoha area (Fig. 5-1, Table 6.1).

Muine Zone, about 10 km by 6 km in plan size, occurs in and around the Muine volcano. This zone is characterized by sporadic occurrences of advanced argillic alteration near the phreatic craters and extinct fumaroles in the Muine Formation, and smectite alteration on the fringe of the Muine Formation (Fig. 5-1, Table 6-1). The advanced argillic alteration is hosted by hydrothermal breccia (Fig. 6-1a), massive andesite dykes (Fig. 6-1b), and lacustrine sedimentary rocks (Fig. 6-1c). Vuggy silica (Figs. 6-1b and c) and massive silicification (Fig. 6-1d) with waxy surface, formed by cristobalite and tridymite, are common. Alunite is generally cryptocrystalline and is associated with cristobalite and tridymite, but phanero-crystalline alunite occurs exceptionally in a quartz-junitite-pyrite alteration zone five meters thick at the upstream of the Hiramizugawa River. Arsenic occurrences are included within the smectite alteration zone.

Toyoha Zone, 4 by 2.5 km in size, fringes the ore veins of the Toyoha deposit (Fig. 5-1). The alteration zone is thickest in the mine site (>800 m) and decreases in thickness to about 300 m near the eastern margin of the zone (Shimizu and Aoki, 2001b). The host rocks of this zone are Middle-Early Miocene andesite and sedimentary rocks. The alteration zone is divided into upper argillic and lower propylitic and sericitic alteration (Fig. 6-2, Table 6-1). The propylitic-sericitic alteration changes in assemblage from quartz-illite-pyrite to quartz-chlorite-calcite-albite or K-feldspar as the distance from the ore veins increases (Fig. 6-2; Sawai, 1984). Kaolinite and dickite, and occasionally pyrophyllite, overprint on the quartz-illite-pyrite assemblage associated with the veins in the southwestern part of the Toyoha zone (Sawai, 1984; Sanga et al., 1992). These minerals precipitated from the descending acid solutions formed in the steam-heated environment near the surface. A quartz-epidote-K-feldspar assemblage becomes dominant at the southern margin of the deposit where the present rock temperature exceeds 100°C (Fig. 6-2; Masuda et al., 1996).

Three end member chlorites occur in the Toyoha zone. Iron-rich chlorite with fluorine apatite (Sawai, 1984; Ohta and Marumo, 1985) occur as gangue minerals in the ore veins of the Toyoha zone, whereas manganese-rich chlorite occurs in the ambient part of the vein system. Chlorite in the host rocks without the influence of the ore fluid is depleted in iron and manganese. Gangue chlorite from Pb-Zn veins, chlorite from manganese-carbonate veins and chlorite from alteration haloes form the periphery of the Toyoha zone plot within the triangle defined by the three end members in the Fe/(Fe+Mg+Mn) versus Mn/(Fe+Mg+Mn) diagram (Fig. 6-3). This distribution is interpreted as that the chlorite formed by the mixing of hypogene ore solution and geothermal water, and/or the reactions between hypogene ore solution with host rocks, and between geothermal fluid with host rocks.

Table 6-1 Hydrothermal minerals in the Muine, Toyoha and Yunosawa zones. Red: ubiquitous, orange: common, blue: uncommon.

Alteration zone	Planar size	Vertical thickness	Location	Alteration type	Alteration minerals
Muine	10 x 6 km	>400 m	Volcanic center	Advanced argillic (center)	alunite, cristobalite, tridymite, pyrite, limonite, quartz, kaolinite, dickite, pyrophyllite, barite, cinnabar
				Argillic (margin)	smectite, cristobalite, pyrite, kaolinite, realger, orpiment
Toyoha	4 x 2.5 km	>800 m	Fracture zones	Argillic (upper)	cristobalite, smectite, smectite/chlorite interstratified clay, smectite/illite interstratified clay, kaolinite, quartz
				Propylitic (lower)	chlorite, illite, pyrite, quartz, calcite, albite, K-feldspar, epidote, kaolinite, dickite, pyrophyllite
Yunosawa	2 x 1 km	300 m	Extension of fracture zones	Advanced argillic-argillic, silicification	cristobalite, quartz, kaolinite, alunite, smectite/illite interstratified clay, pyrite, illite, dickite, native sulfur, pyrophyllite, rutile

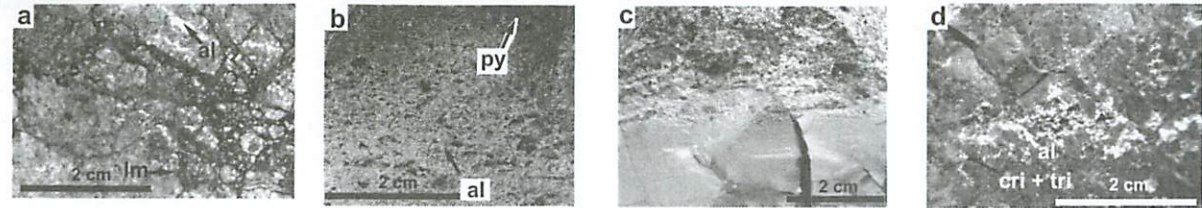
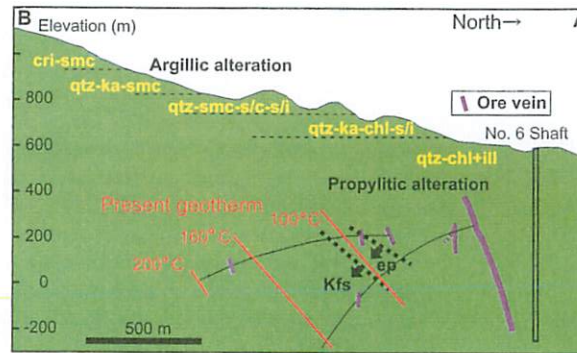


Fig. 6-1 Photographs showing the occurrence of altered rocks in the Muine zone. **a:** Hydrothermal breccia cemented with limonite (lm). Alunite (al) occurs as veins and replacement of feldspar. **b:** Acid-leached andesite lava. Euhedral alunite occurs in vugs and microcrystalline pyrite (py) is disseminated in the upper part of the photo. **c:** Acid-leached sandstone and mudstone with stratification. Both the lower massive and upper vuggy parts consist of cristobalite. Barite and alunite occur in vugs. **d:** Massive cristobalite-tridymite rock with alunite, originated from andesite.



	vein	wall rock
alb/Kfs		
cal		
chl		
qtz		
ill		
py		

Fig. 6-2 North-south section showing mineral assemblages in the southern Toyoha zone (upper) and change of the mineral assemblage near the ore veins (Sawai, 1984). See the A-B section in Fig. 5-1. Abbreviations are; chl: chlorite, cri: cristobalite, ep: epidote, ill: illite, ka: kaolinite, Kfs: K-feldspar, qtz: quartz, smc: smectite, s/c: smectite/chlorite interstratified clay, and s/i: smectite/illite interstratified clay.

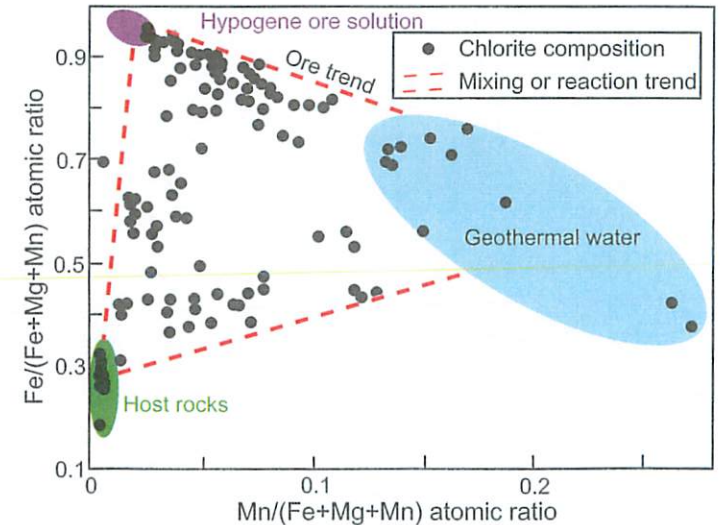


Fig. 6-3 Chemical compositions of chlorite from peripheral veins in the southern and southeastern parts of the Toyoha zone. The three areas labeled as hypogene ore solution, geothermal fluid and host rocks represent compositions of chlorite in equilibrium with these three phases, respectively. The area with red broken line is mixing or reaction trends between these the corresponding phases.

The Yunosawa Zone is exposed in a 2 x 1 km area along the northwest trend of the Yunosawa River, corresponding to the area of present high rock temperature (Fig. 6-4; NEDO, 1988). This zone is 300 m thick and was formed in steam-heated environment near the paleo surface. Advanced argillic assemblage mixed with argillic assemblage (Table 6-1) is widespread on the surface. Quartz-dickite, and cristobalite-alunite assemblages (Fig. 6-5a) occur at the places where the fractures that host the major veins of the Toyoha deposit crosscut this alteration zone (Figs. 5-1 and 6-4). Dickite becomes dominant at depth and pyrophyllite occurs at the base of this zone (NEDO, 1988). The cristobalite-alunite area includes a sulfate-rich low-temperature fumarole with a halo of cristobalite and sublimation sulfur.

The Yunosawa zone also contains an 300 m by 200 m area of massive silicification, consisting of vuggy and massive quartz formed by acid leaching and silicification, respectively. The massive part includes breccia and a layered silica sinter (Fig. 6-5b) with desiccation cracks and potholes (Fig. 6-5c). Coexistence of vapor-dominant inclusions with liquid-dominant ones in the quartz veins intruding vuggy and massive quartz indicates fluid boiling at a temperature of 170°-180°C about 75-80 m below the paleo water table (Shimizu and Aoki, 2001a).

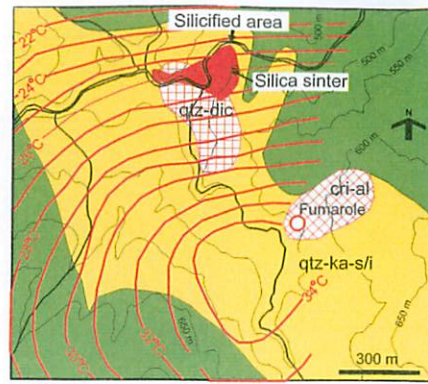


Fig. 6-4 Yunosawa alteration zone (yellow) with areas of cristobalite-alunite, quartz-dickite and silicification. Geotherm contours at the depth of 30 m (NEDO, 1988) are plotted.

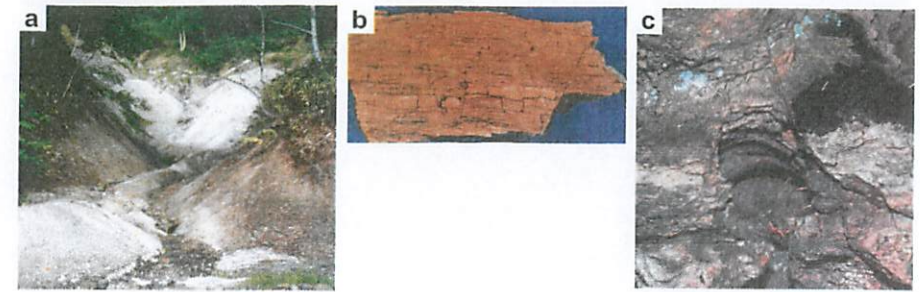


Fig. 6-5 Photographs showing hydrothermally altered rocks in the Yunosawa zone. **a:** Cristobalite-alunite area in the Yunosawa zone. **b:** Layered quartz from the silica sinter. **c:** Potholes in the silica sinter.

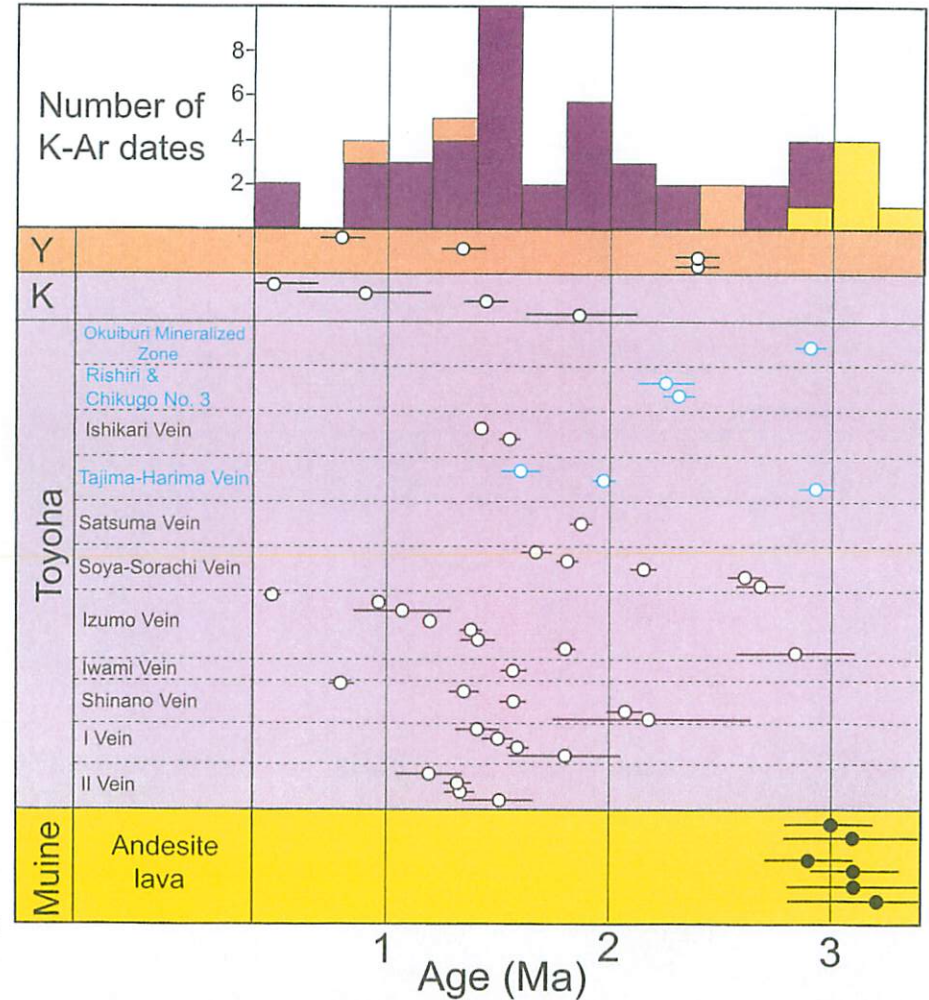
7) Temporal relationship

K-Ar dates of the andesite of the Muine Formation, hydrothermal illite associated with ore veins in the Toyoha and Kurumizawa zones, and hydrothermal illite in the Yunosawa zone indicate a temporal relationship among the volcanism, mineralization and hydrothermal alteration (Fig. 7-1).

The andesitic volcanism at the Muine volcano at 3.2-2.9 Ma was followed immediately by the hydrothermal activities at the Toyoha zone. These hydrothermal activities continued over two million years. The temporal relationship between the volcanic activity at Muine and mineralization in the Toyoha deposit, present and paleo-geotherm gradients that increase in temperature towards the southeast in the Toyoha deposit (Ohta, 1991) and the presence of the extremely conductive zone interpreted as hydrothermal reservoir and/or melted magma beneath the Muine volcano (Takakura and Matsushima, 2003) suggest that hydrothermal mineralization at Toyoha was not directly related to the magmatic eruptions of the Muine volcano, but was related to the non-eruptive intrusive activities beneath the Muine volcano. K-Ar dates of the Toyoha zone are not apparently consistent with the division of early and late mineralization stages. This may be due to the overprint on the early-stage mineralization by the late-stage one, which makes distinct stage identification difficult (Ohta, 1991). Among these K-Ar dates, the veins in the northern part of the deposit (Okuiburi, Rishiri and Chikugo No. 3) yield relatively older dates (2.9-2.3 Ma), whereas veins in the south (Shinano, I and II) have relatively younger dates (2.2-0.8 Ma). Veins in the middle part of the deposit (Tajima, Harima, Soya, Sorachi and Izumo) are variable in date (2.9-0.5 Ma).

The scattered age dates in the Yunosawa zone suggest that the hydrothermal activities of the zone were not single, but multiple. This is supported by the inconsistent presence of illite in the smectite-kaolinite alteration assemblage and quartz veins in the acid-leached cristobalite rocks near the fumarole of the alteration zone. The scattered illite dates of the Yunosawa zone are, nevertheless, included in the time range of the hydrothermal activities in the Toyoha zone. This suggests that the hydrothermal alteration at Yunosawa was also related to the hydrothermal activities in the Toyoha zone.

Fig. 7-1 K-Ar dates of the andesite of the Muine Formation, and hydrothermal illite associated with ore veins in the Toyoha (Sawai et al., 1989; Masuda et al., 1996) and Kurumizawa zones (K: Shimizu and Aoki, 2001b) and hydrothermal illite in the Yunosawa zones (Y: Sawai et al., 1989; Ministry of International Trade and Industry, 1999). Veins with blue and brown colors are the early- and late-stage ones, respectively.



8) Vein system

The Toyoha deposit consists of three major vein systems; east-striking veins of Tajima, Harima, Izumo, and Shinano, northwest-striking Soya and Ishikari veins, and north-striking Sorachi and Rebun veins (Fig. 8-1). These veins are distributed within an area of about 3 km by 2.5 km and are developed as deep as 600 m from the surface. These veins generally dip towards the center of the vein system, represented by the north-dipping Tajima, Harima and Izumo veins in the central and southern parts of the deposit and the south-dipping Nagato, Chikugo No. 2, and Chikugo No. 3 veins in the northern part of the deposit (Fig. 8-1). The veins in the central and northern parts of the deposit crop out on the surface, whereas those in the southern part are not exposed. The major east-striking veins, Tajima, Harima and Oshima-Shitaban, step over to each other, forming cymoid loops at the junctions (Fig. 8-2a).

The veins of the Toyoha deposit are divided into an early stage and a late stage, based on the cutting relations between the veins and ore mineral assemblages (Figs. 8-2b and c; Akome and Haraguchi, 1967). The major trends of the early-stage and late-stage veins are shown in Figs. 3-4. The fractures that host the most east, north-northwest and northwest-striking veins of the early stage are regarded to be right-lateral strike-slip, left-lateral strike-slip and tensional in origin, respectively, based on (1) the displacement of the geologic unit along the veins, (2) echelon alignment of folds along the veins, and (3) change of the strike of the Miocene sedimentary rocks towards the veins (Fig. 8-3; Watanabe, 1990b; Watanabe and Ohta, 1995). The stress orientation estimated from this vein assemblage is $N60^{\circ}W$ compressional and $N30^{\circ}E$ tensional (Fig. 8-4). A depression structure formed by east-striking veins of the early stage (Kuwahara et al., 1983) is interpreted by the right-lateral strike-slip faulting along these vein fractures (Watanabe, 1990b).

The late-stage veins consist of the veins with west-northwest, north, north-northwest and east-northeast trends. The fractures that host the west-northwest, north, and north-northwest veins are regarded as right-lateral, left lateral and tensional in origin, based on the displacements of the early-stage veins by the late ones. The stress orientation estimated from this vein assemblage is $N30^{\circ}W$ compressional and $N60^{\circ}E$ tensional (Fig. 8-4). The east-northeast striking Satsuma and NE-Shinmyaku veins are regarded to be compressional in origin, because these veins are situated on the echelon fold axes, which formed along the major east-striking Tajima and Harima veins of the early stage. These fold axes may have been fractured by the later $N30^{\circ}W$ compressional stress.

The west-northwest and northwest-striking vein fractures of the early stage were reactivated during the late mineralization period, whereas the east-striking veins of the early stage were not. This may be due to the large angle ($>60^{\circ}$) between the orientation of the compressional stress during the late stage and the east-striking fractures, which made difficult for these veins to be reactivated.

The change of the compressional stress orientation estimated in the Toyoha deposit is concordant with the change of the regional stress field, represented by the orientations of volcanic chains in the Sapporo-Iwanai district (Watanabe, 1993), as well as that of the Hawaiian volcanic chain, which represents the subduction direction of the Pacific plate (Jackson et al., 1975).

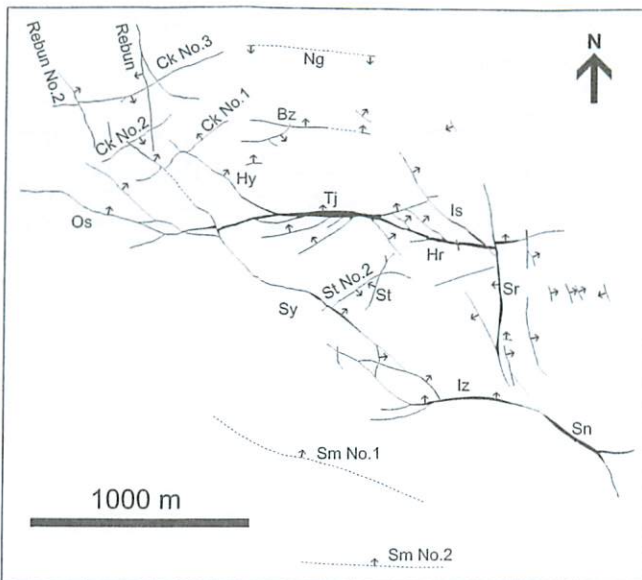


Fig. 8-1 Vein map of the Toyoha deposit (plan view). Arrows on the veins show dip direction. Abbreviation for the veins are; Bz: Bizen, Ck: Chikugo, Hy: Hiyama, Is: Ishikari, Iz: Izumo, Ng: Nagato, Os: Oshima-Shitaban, Rb: Rebun, Sn: Shinano, Sr: Sorachi, and St: Satsuma.

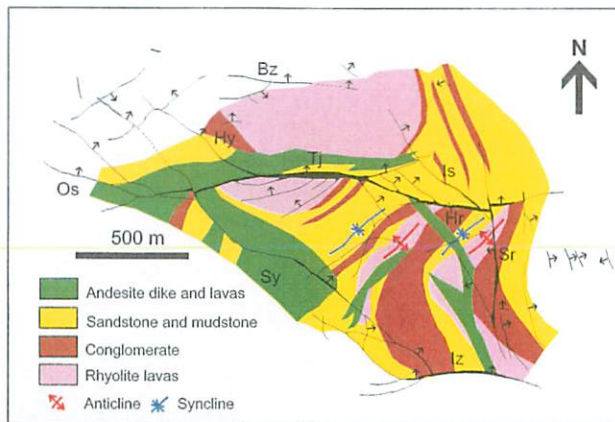


Fig. 8-3 Geological map of the Toyoha deposit simplified from Watanabe (1990b). Rhyolite lavas of the Shiramizugawa Formation north of the Tajima vein form a lava dome, of which southern margin was cut and displaced. The conglomerate unit and sandstone and mudstone unit were also deformed, resulting in the change of the strikes from northwest to northeast towards the major veins and en echelon folding. All these deformation structures indicate right-lateral strike-slip movement along the major east-striking veins.

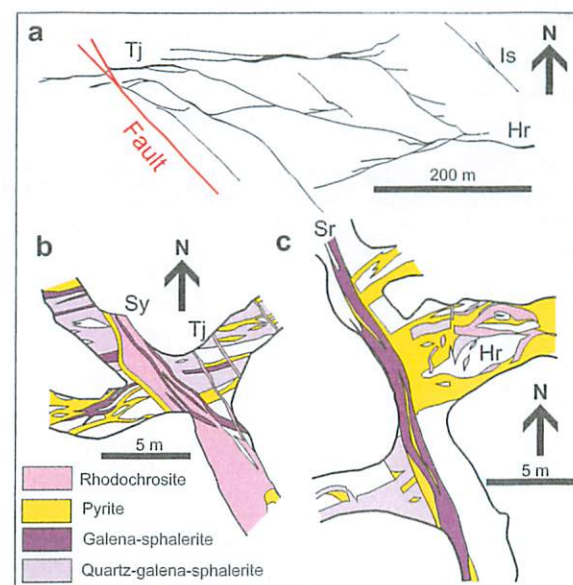


Fig. 8-2 Relationship between veins. a: Cymoid loop at the junction of Tajima and Harima veins at -300 m (Miyajima et al., 1971). b: Tajima vein cut by Soya vein (Akome and Haraguchi, 1967). c: Harima vein cut by Sorachi vein (Akome and Haraguchi, 1967).

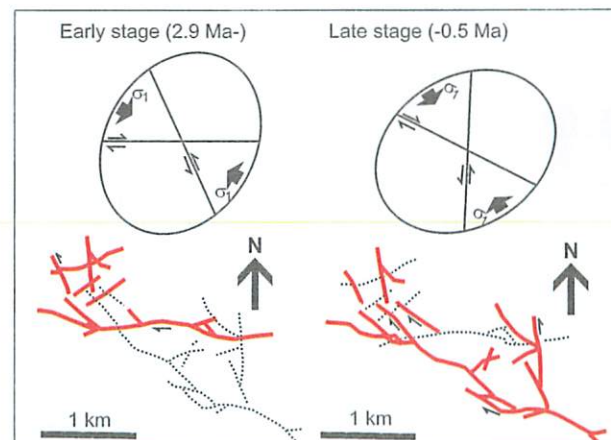


Fig. 8-4 Stress fields during the early and late stage mineralization, based on the sense of faulting (Watanabe and Ohta, 1995). Early and late stage veins are shown in red. Arrows indicate sense of shear. Pair of solid arrows indicate the direction of the maximum compressional stress (σ_1).

9) Ore-forming stages

In spite of the production of limited metal commodities, the Toyoha deposit yields a variety of ore minerals including rare metals such as tin, indium, tungsten, cobalt, nickel, bismuth, selenium, tellurium, etc. Detailed studies on mineral paragenesis revealed that the ore-forming process of the Toyoha deposit is divided into the early and late stages, and the late stage is further subdivided into five substages (Ohta, 1991; Fig. 9-1).

The early-stage mineralization is characterized by a simple mineral assemblage of iron-poor sphalerite, galena and pyrite. Hematite is commonly observed in this assemblage, in particular, in the veins of the northwestern part of the deposit (Yajima and Ohta, 1979; Ohta, 1991). Parts of hematite were replaced by magnetite during the Substages B, C, and D of the late stage.

The late stage is subdivided into substages A, B, C, D and E (Ohta, 1989, 1991). Substage A is characterized by the assemblage of iron-rich sphalerite, pyrite and pyrrhotite.

Substage B is characterized by tin and indium minerals, associated with chalcocopyrite, sphalerite, galena, wolframite and arsenopyrite. Cobalt and nickel occur mainly as cobaltite-arsenopyrite solid solution that intergrows as bands within arsenopyrite. An unnamed Zn-In mineral occurs within sphalerite (Fig. 9-2). This mineral has a chemical composition at the midst of sphalerite and roquesite (Fig. 9-3). Stannite, kesterite and chalcocopyrite often accompany it. Bismuth occurs at deep levels of the veins in the southeastern part of the deposit. Complex microscopic aggregates of several Ag-Pb-Bi minerals are observed in the chalcocopyrite-rich ore. Bismuth minerals include native bismuth, bismuthinite, a gustavite-like phase, matildite, a matildite-galena solid solution, and unknown phases whose chemical compositions are between gustavite and the matildite-galena solid solution (Ohta, 1992).

Substage C is characterized by silver sulfosalts such as pyrargyrite, diaphorite and freibergite, associated with galena and sphalerite. Argentite constitutes sporadic silver-rich zones in the early-stage veins (Ohta, 1992). Hocartite occurs in this substage due to a reaction between tin minerals of Substage B and the silver-rich hydrothermal solution of this substage. An unnamed Ag-In mineral is rarely and locally recognized at middle to upper levels of the Sorachi vein where intense silver mineralization followed that of tin and indium. Cassiterite, which formed during Substage B, were modified into canfieldite or other tin sulfides during this substage.

Substage D is recognized mainly in northern half of the Soya vein. Sphalerite and galena in this substage are not associated with silver, tin or indium minerals. Dickite is common. Decomposition of pre-existing tin sulfides occurred due to oxidation during this substage. Silver sulfosalts that formed during Substage C were modified into Pb-Sb sulfosalts. Toyohaite, Ag-dominant analogue of rhodostannite, was discovered in the lower levels of the central part of the Sorachi vein. Although toyohaite is included in Substage B ore, it formed during this substage with rhodostannite and hocartite, by replacing stannite that formed during Substage B (Yajima et al., 1991; Ohta, 1992).

Substage E is recognized mainly in the northwestern part of the deposit. This substage is characterized by manganese minerals. Native silver formed during this substage by decomposition of argentite (Ohta, 1992).

Stage Sub-stage	Early		Late				
			A	B	C	D	E
Sphalerite (ZnS)	Major	Major	Major	Major	Major	Major	Major
Galena (PbS)	Major	Major	Major	Major	Major	Major	Major
Pyrite (FeS ₂)	Major	Major	Major	Major	Major	Major	Major
Hematite (Fe ₂ O ₃)	Major	Major	Major	Major	Major	Major	Major
Pyrrhotite (FeS)	Major	Major	Major	Major	Major	Major	Major
Cassiterite (SnO ₂)	Major	Major	Major	Major	Major	Major	Major
Stannite (Cu ₂ FeSnS ₄)	Major	Major	Major	Major	Major	Major	Major
Wolframite [(Fe,Mn)WO ₄]	Major	Major	Major	Major	Major	Major	Major
Chalcocopyrite (CuFeS ₂)	Major	Major	Major	Major	Major	Major	Major
Arsenopyrite (FeAsS)	Major	Major	Major	Major	Major	Major	Major
Co minerals	Major	Major	Major	Major	Major	Major	Major
Bi minerals	Major	Major	Major	Major	Major	Major	Major
Tennantite [(Cu,Ag,Fe,Zn) ₁₂ As ₄ S ₁₃]	Major	Major	Major	Major	Major	Major	Major
Tetrahedrite [(Cu,Fe,Ag,Zn) ₁₂ Sb ₄ S ₁₃]	Major	Major	Major	Major	Major	Major	Major
Argentite (Ag ₂ S)	Major	Major	Major	Major	Major	Major	Major
Ag sulfosalts	Major	Major	Major	Major	Major	Major	Major
Berthierite (FeSb ₂ S ₄)	Major	Major	Major	Major	Major	Major	Major
Pb-Sb sulfosalts	Major	Major	Major	Major	Major	Major	Major
Rhodochrosite (MnCO ₃)	Major	Major	Major	Major	Major	Major	Major
Rutile (TiO ₂)	Major	Major	Major	Major	Major	Major	Major
Quartz (SiO ₂)	Major	Major	Major	Major	Major	Major	Major

— Major amount — Minor amount

Sn & In minerals (Substage B)
Cassiterite (SnO ₂)
Herzenbergite (SnS)
Berndtite (SnS ₂)
Teallite (PbSnS ₂)
Stannite (Cu ₂ FeSnS ₄)
Kesterite (Cu ₂ ZnSnS ₄)
Pirquitasite (Ag ₂ ZnSnS ₄)
Rhodostannite (Cu ₂ FeSn ₃ S ₈)
Zn-In mineral (CuZn ₂ InS ₄)
Roquesite (CuInS ₂)
Sakuraiite [(Cu,Fe,Zn) ₃ (In,Sn) ₄ S ₄]
Ag minerals (Substage C)
Ag-In mineral (AgInS ₂)
Argentite (Ag ₂ S)
Canfieldite (Ag ₈ SnS ₆)
Te-canfieldite [Ag ₈ Sn(S,Te) ₆]
Diaphorite (Pb ₂ Ag ₃ Sb ₃ S ₈)
Electrum (Au,Ag)
Gustavite (AgPbBiS ₆)
Hessite (Ag ₂ Te)
Hocartite (Ag ₂ FeSnS ₄)
Miargyrite (AgSbS ₂)
Native silver (Ag)
Owyheeite (Pb ₅ Ag ₂ Sb ₅ S ₁₅)
Pirquitasite (Ag ₂ ZnSnS ₄)
Polybasite [(Ag,Cu) ₁₆ (Sb,As) ₂ S ₁₁]
Pyrargyrite (Ag ₃ SbS ₃)
Toyohaite (Ag ₂ FeSn ₃ S ₈)

Fig. 9-1 Mineral paragenesis of the Toyoha deposit (Ohta, 1991) with lists of tin and indium minerals of Substage B (Ohta, 1989) and silver minerals of Substage C (including some minerals of Substages D and E) (Ohta, 1992).

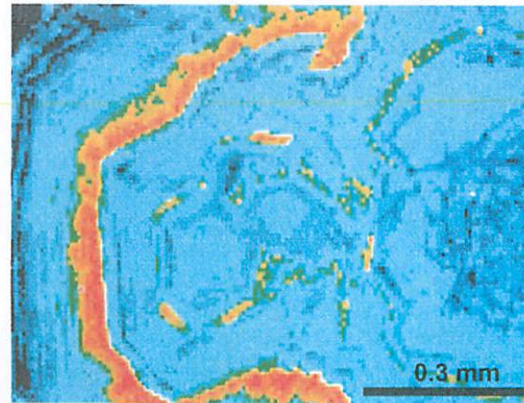


Fig. 9-2 Compositional map showing the distribution of indium in sphalerite (Ohta, 1989). Red and orange color areas and blue color areas are high and low in indium content, respectively.

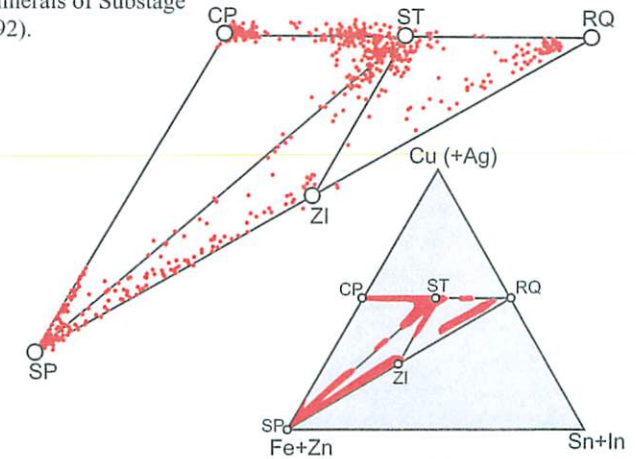


Fig. 9-3 Diagram showing compositions of solid solutions of the chalcocopyrite-sphalerite-roquesite minerals (Ohta, 1995). CP: chalcocopyrite, ST: stannite/kesterite, RQ: roquesite, SP: sphalerite, ZI: zinc-indium sulfide.

10) Ore solution chemistry

Observation of fluid inclusions in sphalerite and quartz from the veins in the Toyoha deposit indicates that the majority of fluid inclusions are liquid-rich two-phase ones under a room temperature (Yajima and Ohta, 1979). These fluid inclusions homogenize into the liquid phase when they are heated. Measurement of homogenization and freezing temperature of these inclusions indicates that the ore solutions were between 310°C and 170°C, with salinities between 0.2 and 9 wt. percent NaCl equivalent at the time of ore deposition in major veins (Fig. 10-1). The results also indicate that the homogenization temperatures and salinities of the late stage (320-200°C, 9-0.7 wt %) are relatively higher than those of the early stage (250-170°C, 2.2-0.2 wt %) (Yajima and Ohta, 1979). The range of the homogenization temperatures of the inclusions in sphalerite are similar to that in quartz, whereas the salinity in sphalerite is higher than that in quartz. The positive homogenization temperature-salinity trend (Fig. 10-1) and the linear trend of data in the enthalpy-salinity diagram (Fig. 10-2) indicate that the ore deposition occurred by the mixing between relatively high-temperature and high salinity solutions with low-temperature and low-salinity fluids, which may represent steam-heated water or meteoric water.

Fluid boiling is suggested locally by the vein texture that changes from lower sulfide ore to upper illite-rich clay through breccia in the Shinano vein (Sanga et al., 1992) and the co-existence of vapor-rich and liquid-rich inclusions in quartz from the Nagato vein (Shimizu and Aoki, 2001a). However, sulfide deposition occurred prior to the boiling, and thus, the ore deposition is triggered by the abrupt decrease of salinity due to fluid mixing (Ohta, 1991; Sanga et al., 1992).

Homogenization temperatures were measured only for fluid inclusions in coarse crystals of quartz and sphalerite. Both of them are rare in the late-stage veins, and formed mostly at Substage C or later. Iron-zinc partitioning temperatures for sphalerite-stannite pairs, and some uncommon phases such as chalcopyrite-stannite solid solutions indicates that the temperature of initial ore solution responsible for the rare-metal mineralization was as high as 400°C (Ohta, 1989, 1991). This suggests that the Toyoha deposit is not a simple epithermal deposit, but has a characteristic of a xenothermal deposit.

Sulfur fugacity-temperature trends of the ore solutions for the early- and late-stage mineralization are estimated based on mineral assemblages, FeS mol percent in sphalerite and homogenization temperatures of fluid inclusions. The stability field of the early-stage ores is situated between $Cu_5FeS_4+FeS_2-CuFeS_2$ and $Fe_2O_3+FeS_2-Fe_3O_4$ boundaries with a slight deviation to pyrite-arsenopyrite boundary (Yajima and Ohta, 1979). That of Substages A is lower than the pyrrhotite-pyrite boundary, and as low as the isopleth of 30 mol percent FeS in sphalerite. Substage B is higher than that in Substage A, and lower than the arsenopyrite-pyrite+arsenic boundary during Substage C. The sequence from Substage A to C indicates increasing sulfur fugacity and/or decreasing temperature (Ohta, 1991; Fig. 10-3).

The early and late stage trends on the temperature- f_{S_2} diagram correspond to the trends of ore solutions derived from magnetite-series and ilmenite-series granitoids (Tsukimura et al., 1987), respectively, and the intermediate trend and low-sulfidation trend for porphyry-related base-metal veins, respectively (Einaudi et al., 2003). This concordance and common existence of tin and indium in the late-stage veins suggest that the late-stage ore solutions derived from a reduced magma.

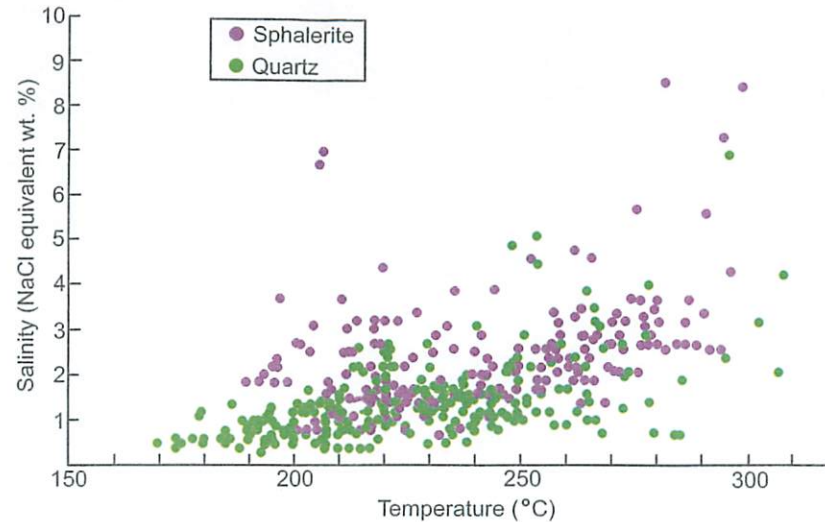


Fig. 10-1 Plots of homogenization temperature vs. salinity for fluid inclusions in sphalerite and quartz from the Toyoha deposit. Data sources are Yajima and Ohta (1979), Sanga et al. (1992), Ono and Sato (1994) and Masuda et al. (1996).

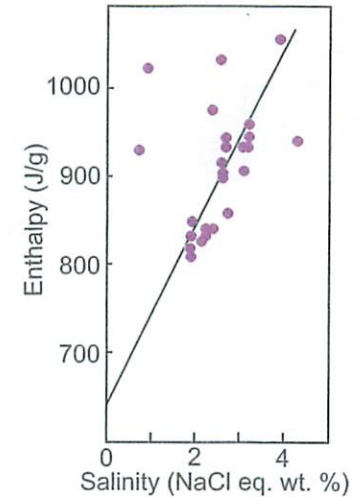


Fig. 10-2 Plots of enthalpy vs. salinity for fluid inclusions in sphalerite from the Reibun vein (Ono and Sato, 1994).

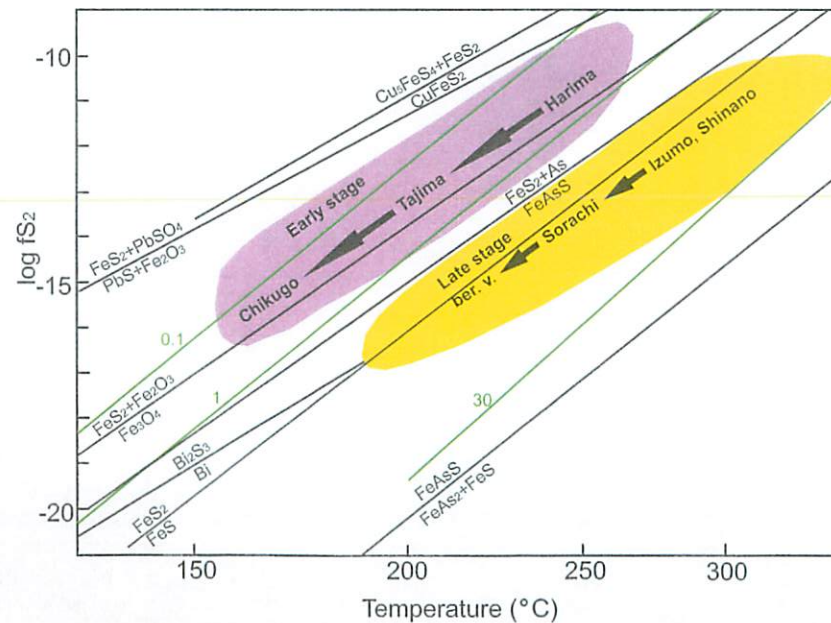


Fig. 10-3 Diagram showing the temperature-sulfur fugacity (f_{S_2}) trends of the ore solutions in the Toyoha deposit (Ohta, 1991). ber. v.: berthierite veins cutting the Tajima vein. Arrow linking the vein names indicate representative flow paths of the ore solutions. Green color lines with numerals are isopleths of FeS mol percent in sphalerite.

11) Hydrothermal environments and fluid origin

In the Muine alteration zone, sulfur isotopic ($\delta^{34}\text{S}_{\text{V-CDT}}$) values of alunite are quite variable, from -4.1 to 31.5 permil, although the majority of data are between 9 and 19 permil (Fig. 11-1). There is a slight variation in individual phreatic craters and extinct fumaroles; 9.1-15.9 permil in the Konuma, Ohnuma and Usubetsu craters, 15.3 and 16.7 permil in an extinct fumarole located between Muine and Nakadake, 17.4-21.5 permil in the Nagaoyama and Daijagahara craters, and 26.7 and 31.1 permil in the Shiramizugawa crater. Two $\delta^{34}\text{S}_{\text{V-CDT}}$ values of pyrite coexisting with alunite are 0.4 permil and -18 permil, giving isotopic equilibrium temperatures of 249°C and 173°C, respectively. The $\delta^{34}\text{S}_{\text{V-CDT}}$ values of orpiment in the Shiramizugawa and Usubetsu occurrences are 3.4 and -5.2 permil, respectively.

Among the broad range of the sulfur isotopic values of alunite in the Muine zone, the alunites heavier than 20 permil are ascribed to the disproportionation of SO_2 to H_2SO_4 and H_2S . An isotopic equilibrium temperature calculated from a pair of alunite and pyrite is included within the typical temperature range (400-200°C) of the magmatic-hydrothermal environment (Rye et al., 1992; Rye, 1993). The alunites with relatively low (9-17 permil) isotopic values from the Ohnuma, Konuma and Usubetsu craters are interpreted as magmatic-steam SO_2 origin (Rye et al., 1992; Rye, 1993), because of the similarity of the isotopic range (6.0-16.9 permil; Sakai and Ueda, 1984) of the volcanic SO_2 , emitted from the Holocene Usu volcano in southwest Hokkaido. The -4.1 permil alunite in the Muine zone has the mineral assemblage of halloysite-smectite-alunite, which is different from the alunite-cristobalite-tridymite assemblage of the other samples. This alunite is interpreted as supergene origin, because of the similarity with the sulfur isotopic value of orpiment in the zone.

The sulfur isotopic values of the sulfides in the Toyoha deposit are limited mostly to a narrow range between 4 and 10 permil (7 permil in average), irrespective of the mineral species, veins, sampled elevations, mineralization stages and mineral assemblages. No difference in sulfur isotopic value is recognized between the early- and late-stage sulfides (Fig. 11-1). These sulfide minerals precipitated under disequibrated conditions, suggesting rapid precipitation from supersaturated ore solutions (Hamada and Imai, 2000). These results indicate the predominance of reduced aqueous sulfur species over the oxidized sulfur in the ore solutions throughout the mineralization stage, and suggest magmatic origin for the sulfur (Hamada and Imai, 2000).

The sulfur isotopic value, -2.8 permil, of alunite, together with 3.2 permil of SO_4^{2-} in the present spring water (NEDO, 1988) indicates atmospheric oxidation of H_2S above the paleowater table in the Yunosawa zone. Despite of the similar alteration mineral assemblages to those of the Muine zone, a steam-heated environment is assigned to the Yunosawa zone, because of the argillic alteration zone limited to a shallow level (<300 m), oxidation of H_2S indicated by the ^{34}S -depleted alunite, and fluid boiling evidence at a low temperature (c. 150°C; Shimizu and Aoki, 2001a).

Oxygen isotopic values for the early- and late-stage ore solutions in the Toyoha deposit have the ranges from -9.2 to -7.3 permil (Tajima and Harima veins) and from -6.5 to -3.2 permil (Sorachi, Izumo and Shinano veins), respectively. These ranges are higher than those of the present surface water and geothermal water. If the oxygen isotopic value of the meteoric water during the mineralization was not significantly different from that of the present-day surface water, the ore solutions may have been formed by mixing of deep-origin fluids with meteoric water, and the contribution of deep-origin fluids was more significant during the late-stage mineralization than during the early-stage mineralization (Matsuhisa et al., 1986).

Oxygen isotope values of the fluids in the quartz-dickite and cristobalite-alunite areas in the Yunosawa zone, determined by quartz analyses, are -10.5 to -10.1 permil and -7.0 to -6.5 permil, respectively (Shimizu and Aoki, 2001a). These two sets of data are significantly different to each other, but are slightly depleted in ^{18}O from the ranges of the Tajima-Harima veins and Izumo-Shinano veins, respectively (Fig. 11-2). This relation suggests that the hydrothermal fluids flowed along E-trending fractures from the Toyoha deposit to the Yunosawa zone, mixing with additional meteoric water.

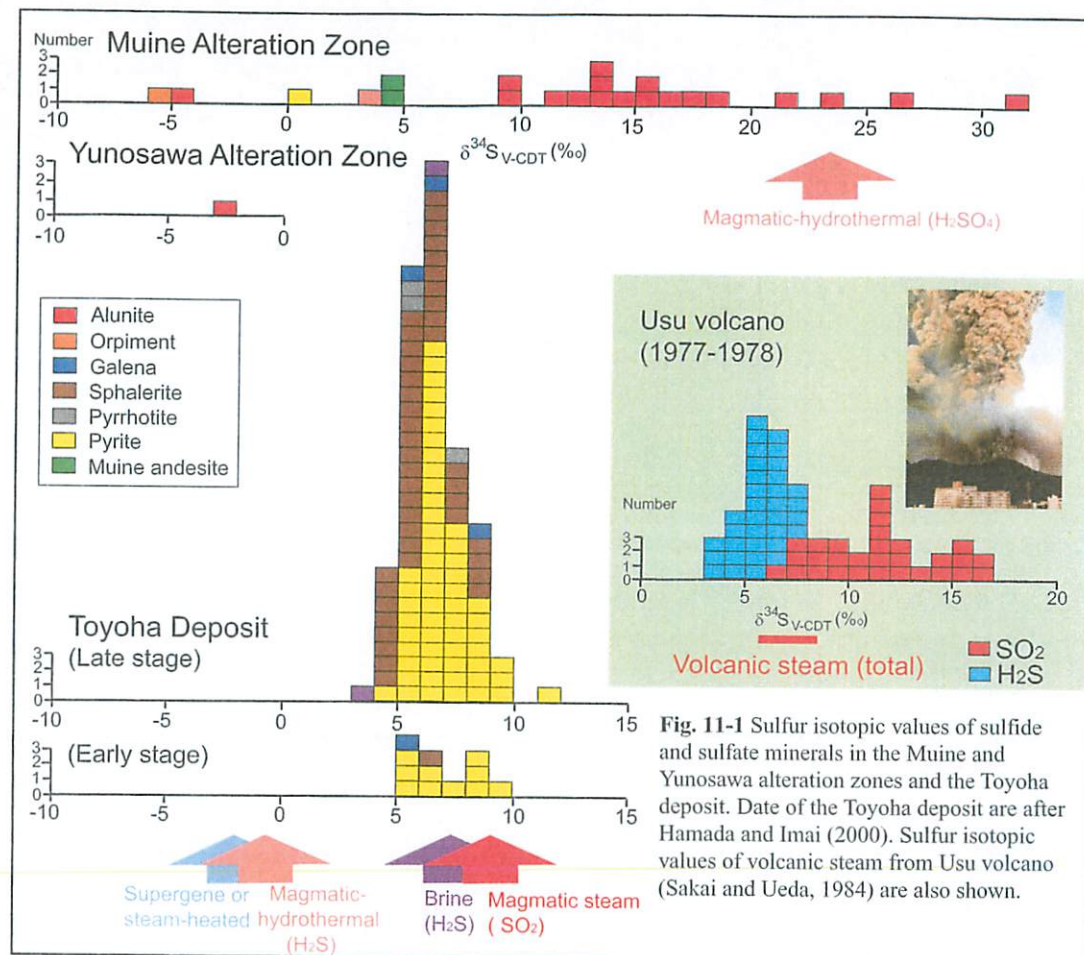


Fig. 11-1 Sulfur isotopic values of sulfide and sulfate minerals in the Muine and Yunosawa alteration zones and the Toyoha deposit. Date of the Toyoha deposit are after Hamada and Imai (2000). Sulfur isotopic values of volcanic steam from Usu volcano (Sakai and Ueda, 1984) are also shown.

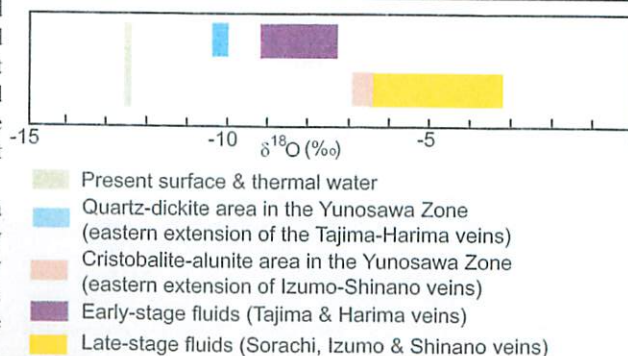


Fig. 11-2 Calculated oxygen isotopic values for the hydrothermal fluids during the early- and late-stage mineralization in the Toyoha deposit (Matsuhisa et al., 1986) and those for hydrothermal fluids in the Yunosawa zone (Shimizu and Aoki, 2001a). Measured oxygen isotopic values of present surface water and thermal water are also shown (See references in Shimizu and Aoki, 2001a).

12) Synthesis

A genetic link between the Toyoha deposit and the magmatic intrusions beneath the Muine volcano is suggested by the presence of the advanced argillic alteration in the Muine volcano and extremely conductive zone beneath the volcano, geochronologic relationship between the volcanism at Muine and hydrothermal activities at Toyoha, the present and paleo isotherm structures in the Toyoha deposit that increase in temperature towards the Muine volcano, and stable isotopic signatures of the hydrothermal fluids. These magmatic intrusions occurred subsequent to the eruptions of the Muine andesite lavas at 3.0 Ma, while the tectonic stress in the region was strengthened due to the increase of the orthogonal convergence rate between the Pacific plate and the Northeast Japan arc.

The spatial distribution and nature of the hydrothermal alteration zones indicate that the fluids exsolved from the magmas separated into vapor and brine due to immiscibility (Fig. 12-1) that was inevitable to occur when magma intrudes in the crust to 2-3 km depth (Lowenstern, 1994; Shinohara, 1994). A large density contrast between the vapor and brine resulted in these two phases separating within the magma chamber or its adjacent hydrothermal system (Henley and McNabb, 1978; Bischoff, 1991). The aqueous vapor that contains CO₂, SO₂, H₂S, HCl and other species ascended, and was either discharged to the surface as volcanic fumaroles or absorbed at depth, forming acid fluid that caused the advanced argillic alteration in magmatic-steam or magmatic hydrothermal environments in the Muine alteration zone. The acid fluid flowed in the permeable zone along the contacts of the Pliocene and Miocene formations, and finally neutralized and precipitated smectite and arsenic at the margin of the hydrothermal system (Fig. 12-1).

The brine enriched in silver, lead, zinc, manganese, etc. (Heinrich et al., 1999) flowed laterally to the north, up to the Shiraigawa fault zone, where E-trending strike-slip fractures are present. The impermeable sedimentary rocks of the Usubetsu Formation above the intrusive bodies may have promoted this lateral flow by providing a hydrologic cap to the system. Then the brine ascended through fractures and mixed with meteoric water within the permeable Miocene volcanic rocks above the Usubetsu Formation, as indicated by the fluid inclusion and oxygen isotopic data. This mixing reduced the salinity and temperature of the solutions, resulting in precipitation of base metals in the Toyoha deposit (Ohta, 1991; Sanga et al., 1992).

Boiling of hydrothermal fluids after the deposition of the major sulfide minerals in the Toyoha deposit released vapor including CO₂ and H₂S, which were oxidized above the paleo water table, resulting in the formation of acid water. This acid water caused widespread argillic and advanced argillic alteration near the surface in the Yunosawa and Toyoha alteration zones. A part of acid water descended along the ore veins, modified preexisting sulfide minerals (Substages D and E) and precipitated dickite and pyrophyllite at depth (Fig. 12-1).

High concentration of tin and indium occurred during Substage B of the late-stage mineralization at Toyoha, when the ore solutions were significantly reduced. This is concordant with that highly concentrated tin (hundreds or possibly thousands of ppm) can be transported as reduced Sn(II)-Cl complexes in the fluids that were initially in equilibrium with a high-temperature (>400°C) granitic source (Heinrich, 1990). This temporal reduction of the ore solutions without any change of the sulfur isotopic range at Toyoha suggests that I-type, magnetite-series magma reduced locally into the fo₂ range of the ilmenite series beneath the Muine volcano due to assimilation of organic materials in sedimentary rocks of the Usubetsu Formation. This may have caused by a magmatic intrusion into a shallower level, where the magma intruded the Usubetsu Formation. The shallow-level magmatic intrusion may have been reflected in the high mineralization temperature (350°-400°C) and elevated contribution of deep-origin fluids during Substage B (Fig. 12-2c).

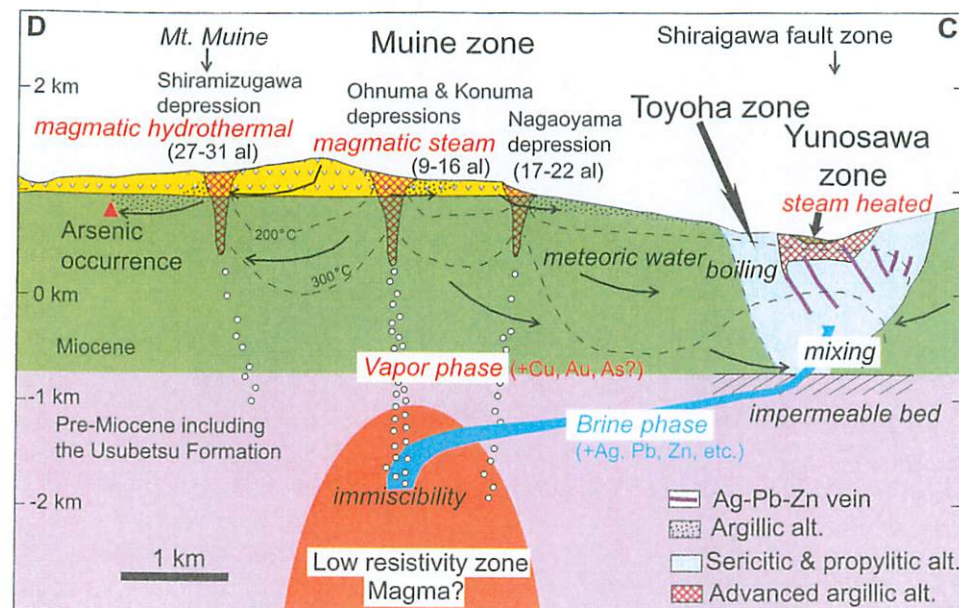


Fig. 12-1 North-south section of the Muine-Toyoha magmatic hydrothermal system. Locations of the low resistivity zone, Yunosawa alteration zone and arsenic occurrence are projected on this section. Number within parenthesis is sulfur isotopic range of alunite. The location of this section (C-D) is shown in Fig. 5-1.

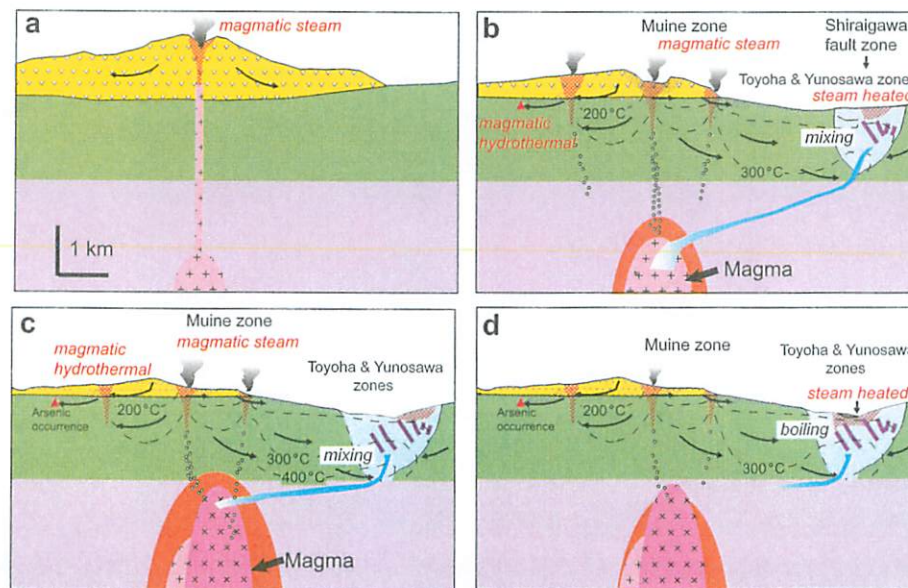


Fig. 12-2 Evolution model of the Muine-Toyoha magmatic hydrothermal system. a: volcanic stage (3 Ma), b: Early-stage mineralization, c: Late-stage mineralization (Substages A & B), and d: Late-stage mineralization (Substages D & E). See pattern captions in Fig. 12-1.

13) Exploration implications

A series of the studies related to the Muine-Toyoha magmatic hydrothermal system provide some exploration implications in differentiating mineralized systems from barren ones and in expecting the locations of the base and precious metal mineralization associated with magmatic hydrothermal systems in calc-alkaline volcanic fields.

(1) Regional tectonic regime: The timing of the metallic mineralization at Toyoha and other major deposits in southwest Hokkaido indicates that the metallic mineralization occurred when the regional tectonic stress normal to the arc-trench system was strengthened due to the increase of the orthogonal convergence rate between the Pacific plate and the Northeast Japan arc. The strengthened tectonic stress can promote an intrusive style of magmatism, which may confine exsolved magmatic fluids in the shallow crustal levels (2-3 km depth) and lead to the fluid separation into immiscible vapor and brine. This tectonic regime is different from the Late Miocene slightly extensional regime in southwest Hokkaido (Figs. 13-1a and 13-2b), which is characterized by rare economic mineralization despite of active calc-alkaline andesitic volcanism (Watanabe, 2002). A minute change of regional tectonic regime may be detected in the changes of the location of volcanic front, style and chemistry of volcanism, dominant direction of volcanic chains and dikes, and sense of faulting.

(2) Polygenetic volcanoes tend to form in a neutral tectonic regime where differential stress in a horizontal plane is little, and monogenetic volcanoes and small polygenetic volcanoes (Fig. 13-1a) form in a large differential stress setting, typical in an extensional tectonic regime (Takada, 1994). The metallic mineralization, including polymetallic one like Toyoha, is associated with a composite polygenetic volcano, where magma intrudes beneath it repeatedly (Figs. 13-1b and 13-2c). These composite polygenetic volcanoes do not exhibit a typical shape of stratovolcanoes, because of the presence of multiple volcanic centers. Magmatic intrusions beneath the volcano form widespread advanced argillic and argillic alteration zones in the volcanic edifices, resulting in the promotion of sector collapse of the volcanic edifices with landslide and debris flow (Sillitoe, 1994; Watanabe, 2003a). A strengthened tectonic stress may also promote crustal thickening, assimilation of crustal materials by mafic magma, and magma homogenization, resulting in the formation of more felsic magma, enriched in light rare-earth elements (Kay et al., 1991; Fig. 13-1b).

(3) Structural setting: Permeable zones, such as active faults, geologic unit boundaries and permeable units existing near the magmatic intrusions become the sites preferable for the passage of hydrothermal fluids, fluid mixing and metallic mineral precipitation. In particular, recognition of strike-slip faults and related secondary extensional fractures helps to expect mineralized locations, because strike-slip faults form dominantly in a neutral tectonic regime (Fig. 13-2c) and are associated commonly with dilational jogs, which enable hydrothermal fluids to ascend (Watanabe, 2002; Richards, 2003). However, the study of the Toyoha vein system indicates that the pre-mineral strike-slip faults and fractures do not host mineralization, unless they were reactivated during the period of the hydrothermal activities (Watanabe and Ohta, 1995). The analysis of regional stress field is required to detect the strikes of the faults and fractures active during the hydrothermal activities.

(4) Hydrothermal setting: Understanding of hydrothermal environments based on geology, occurrence of hydrothermally altered rocks, hydrothermal mineral assemblages, and stable isotopic data makes it possible to expect the site of metallic mineralization. Polymetallic base-metal mineralization is expected in the neutral, reduced hydrothermal environment, characterized by propylitic and sericitic alteration, whereas high-sulfidation epithermal gold and copper mineralization is expected in the magmatic-hydrothermal environment, characterized by advanced argillic alteration near the volcanic centers (Hedenquist, 1995). Steam-heated alteration sometimes suggests the mineralized zones, although it does not always occur above the mineralized zones. Understanding of local hydrology and geologic structures is inevitable to expect the mineralized zones.

(5) Tin-indium mineralization: Tin and indium mineralization at Toyoha was associated with I-type ilmenite-series magma that formed possibly due to the assimilation of sedimentary rocks by the magnetite-series magma near the surface. A typical ilmenite-series magma can exsolve neither sufficient base metals or sulfur to form large sulfide ore deposits. Therefore, local reduction of I-type magnetite-series magmas is essential to form economic tin-indium polymetallic veins (Ohta, 1995).

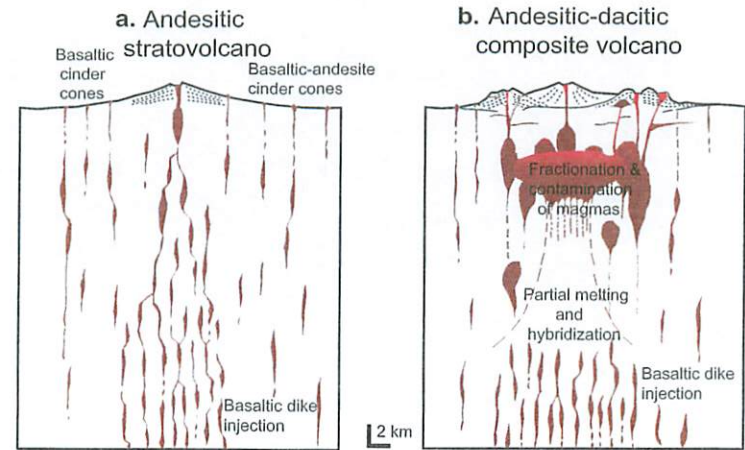


Fig. 13-1 Contrasting styles of volcanoes (Hildreth, 1981). **a:** Andesitic stratovolcano, common in the Late Miocene slightly extensional tectonic regime in southwest Hokkaido. Upward propagation of magma through extensional fractures is realized without significant partial melting and hybridization, resulting in the eruption of relatively mafic magmas. **b:** Andesitic-dacitic composite volcano, common in the Pliocene neutral tectonic regime in southwest Hokkaido. Relatively large magma chambers form due to coalescence of the magma-ascending fractures (Takada, 1994). Partial melting and hybridization form silicic hybrid magmas. An andesite-dacite compositional range develops within magma chambers, primarily by crystal fractionation (Hildreth, 1981).

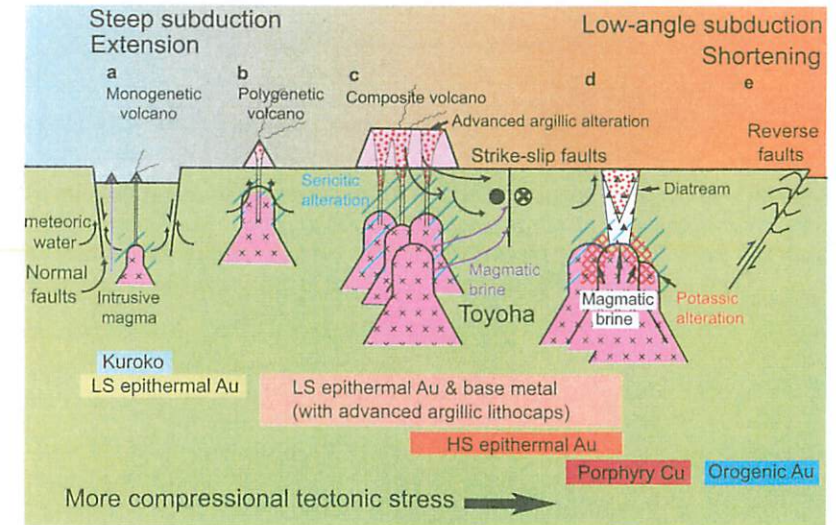


Fig. 13-2 A schematic sequence showing the style of volcanism, faulting and associated deposit type in different tectonic stress (Watanabe, 2003b). Tectonic stress normal to the arc-trench system increases from Stage a to e. Stages a, b and c correspond to the Middle Miocene, Late Miocene and Pliocene tectonic regimes in southwest Hokkaido, respectively. Stages d and e were not realized in southwest Hokkaido. The Toyoha deposit formed in Stage c.

14) Exploration technique

Unknown hydrothermal metallic deposits in the calc-alkaline volcanic fields are not exposed in the surface in general, but may still preserve widespread hydrothermal alteration zones above the deposits. Thus, geophysical and geochemical exploration methods are employed commonly in the exploration for these deposits. Although the Toyoha deposit was discovered from the outcrops of the mineralized veins on the surface, the exploration towards the south of the deposit is not easy because the veins in the southern part of the deposit are not exposed on the surface and the area is covered by landslide deposits. The Metal Mining Agency of Japan tested several exploration techniques to detect unexposed veins in the south of the deposit (Metal Mining Agency of Japan, 1991, 1993).

The CSAMT method detected low resistivity zones along the veins, which are interpreted as the hydrothermal alteration zones rich in hydrous minerals. The other effective method is the GEOGAS method, a kind of gas geochemical exploration methods, which analyzes metals included in the gas ascending from the depth. The analytical results of the samples collected along a north-south section in the southern part of the Toyoha deposit indicate that anomalous base-metal (Cu+Pb+Zn) concentrations occur at the sites where the fractures that host known ore veins are supposed to be exposed on the surface. The results also indicate that some anomalous base-metal concentrations are detected to the south of the known ore veins (Fig. 14-1). These base-metal rich samples also contain anomalous values of potassium and chlorine. The results of soil geochemical prospecting do not show such anomalous base-metal concentrations in these sites. These results indicate that the GEOGAS method is effective to detect unexposed ore veins in such young magmatic hydrothermal systems (Masuda and Tsujimoto, 1991).

Acknowledgements:

We acknowledge the authors of all the papers referred to here for contributing to the understanding of Muine-Toyoha magmatic hydrothermal system. We thank for the past leaders of the exploration section of the Toyoha mine, Keiichi Kumita, Teruo Takeyama and Takashi Yoshie, and the present leader, Eiichi Narui, for allowing us to study the deposit. We are much indebted to Junkichi Yajima, who established early and late mineralization stages of the Toyoha deposit, based on the detailed mineralogical and fluid inclusions studies. This is a part of the results of the research project "Research for development of exploration strategies for large-scale blind ore deposits" of the Institute for Geo-Resources and Environment, AIST from April 2001 to March 2005.



Sorachi vein of the Toyoha deposit with sericite-chlorite alteration halo.

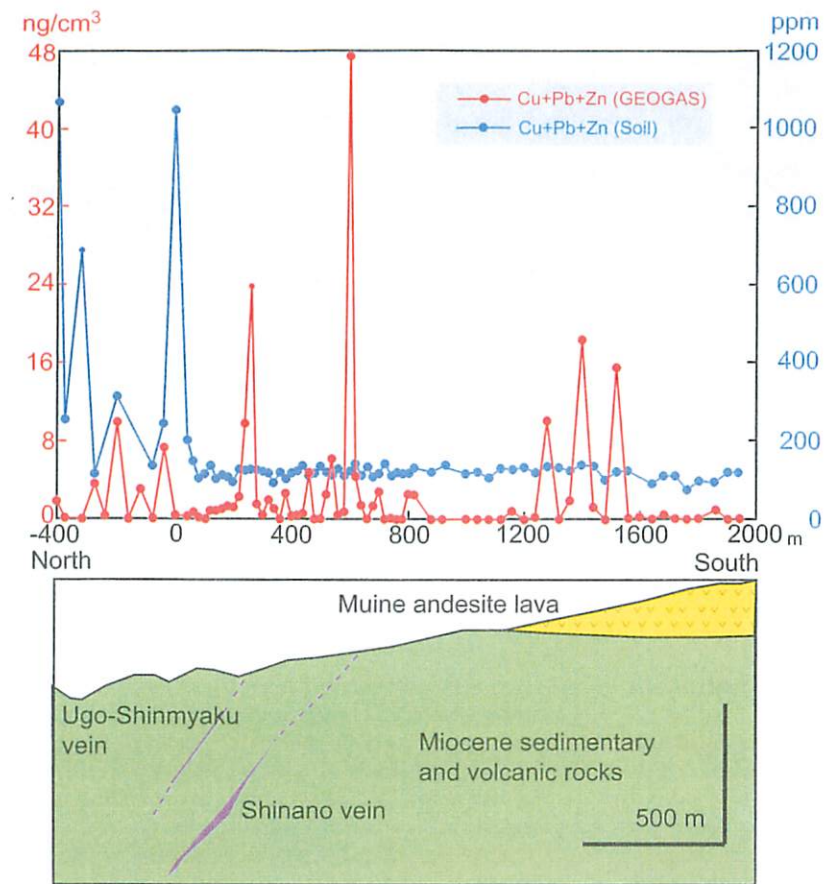


Fig. 14-1 Analytical results of the base-metal (Cu+Pb+Zn) concentrations of the GEOGAS and soil samples along a north-south section in the southern part of the Toyoha deposit after Metal Mining Agency of Japan (1991). Anomalous base-metal concentrations are detected in the GEOGAS samples collected from the surface extensions of the Ugo-Shinmyaku vein and Shinano vein.

References

- Akome, K. and Haraguchi, M. (1967) The characteristics of fracture and mineralization of the Toyoha mine. *Mining Geol.*, 17, 93-100 (in Japanese with English abstract).
- Aoki, M. (1991) Gold and base metal mineralization in an evolving hydrothermal system at Osorezan, Northern Honshu, Japan. *Geol. Surv. Japan Rep.*, 277, 67-70.
- Bischoff, J.L. (1991) Densities of liquids and vapors in boiling NaCl-H₂O solutions. A PVTX summary from 300° to 500°C. *Am. Jour. Sci.*, 291, 309-338.
- Cunningham, C.G., Steven, T.A., Rowley, P.D., Naeser, C.W., Mehnert, H.H., Hedge, C.E. and Ludwig, K.R. (1994) Evolution of volcanic rocks and associated ore deposits in the Marysvale volcanic field, Utah. *Econ. Geol.*, 89, 2003-2005.
- Einaudi, M. T., Hedenquist, J. W. and Inan, E. E. (2003) Sulfidation state of fluids in active and extinct hydrothermal systems: Transition from porphyry to epithermal environments. *Soc. Econ. Geol., Spec. Pub.*, 10, 285-313.
- Fujibayashi, N., Watanabe, Y., Kagami, H. and Kawano, Y. (1995) Temporal and spatial geochemical variation in late Miocene to Pliocene volcanic rocks from the Shakotan Peninsula-Lake Shikotsu area. the northern end of the NE Japan arc. *Mem. Geol. Soc. Japan*, 44, 181-195 (in Japanese with English abstract).
- Hamada, M., and Imai, A. (2000) Sulfur isotopic study of the Toyoha deposit, Hokkaido, Japan- Comparison between the earlier-stage and the later-stage veins-. *Resource Geol.*, 50, 113-122.
- Hedenquist, J.W. (1995) The ascent of magmatic fluid: Discharge versus mineralization. *Mineral. Assoc. Canada, Short Course*, 23, 263-289.
- Hedenquist, J.W., Izawa, E., Arribas, A. Jr. and White, N. (1996) Epithermal gold deposits: Styles, characteristics, and exploration. *Soc. Resource Geol., Spec. Pub. No. 1*, 16p.
- Heinrich, C.A. (1990) The chemistry of hydrothermal tin-tungsten ore deposition. *Econ. Geol.*, 85, 457-481.
- Heinrich, C.A., Gunther, D., Audetat, A., Ulrich, T. and Frischknecht, R. (1999) Metal fractionation between magmatic brine and vapor, determined by microanalysis of fluid inclusions. *Geol.*, 27, 755-758.
- Henley, R.W., and McNabb, A. (1978) Magmatic vapor plumes and groundwater interaction in porphyry copper emplacement. *Econ. Geol.*, 73, 1-20.
- Hildreth, W. (1981) Gradients in silicic magma chambers: Implications for lithospheric magmatism. *Jour. Geophys. Res.*, 86, 10153-10192.
- Jackson, E.D., Shaw, H.R. and Barger, K.E. (1975) Calculated geochronology and stress field orientations along the Hawaiian chain. *Earth Planet. Sci. Lett.*, 26, 145-155.
- John, D. (2001) Miocene and Early Pliocene epithermal gold-silver deposits in the Northern Great Basin, western United States: Characteristics, distribution, and relationship to magmatism. *Econ. Geol.*, 96, 1827-1853.
- Kanbara, H. and Kumita, K. (1990) Mode of occurrence and chemical composition of electrum from the Toyoha polymetallic vein-type deposits, Hokkaido, Japan. *Prof. Urashima volume*, 201-210 (in Japanese with English abstract).
- Kay, S.M., Mpodozis, Ramos, V.A. and Munizaga, F. (1991) Magma source variations for mid-late Tertiary magmatic rocks associated with a shallowing subduction zone and a thickening crust in the central Andes (28 to 30°S). *Geol. Soc. Am., Spec. Pap.* 265, 113-137.
- Kuwahara, T., Miyazaki, T., Tani, T. and Iida, K. (1983) A characterization of the vein mineralizations at the Motoyama deposit, Toyoha mine from the viewpoint of their tectonic setting and ore assays. *Mining Geol.*, 33, 115-129 (in Japanese with English abstract).
- Lexa, J., Stohl, J. and Konecny, V. (1999) The Banska Stiavnica ore district: relationship between metallogenic processes and the geological evolution of a stratovolcano. *Mineral. Deposita*, 34, 639-654.
- Lowenstern, J.B. (1994) Chlorine, fluid immiscibility, and degassing in peralkaline magmas from Pantelleria, Italy: *Am. Mineral.*, 79, 355-369.
- Masuda, K. and Tsujimoto, T. (1991) Application of GEOGAS method to the exploration in Toyoha mine (abstract). *Mining Geol.*, 41, 193 (in Japanese).
- Masuda, K., Kamiki, T. and Narui, E. (1996) Polymetallic mineralization at the Toyoha south district, Hokkaido, Japan. *Resource Geol.*, 46, 45-61 (in Japanese).
- Matsuhisa, Y., Yajima, J. and Ohta, E. (1986) Oxygen-isotope ratio and fluid inclusions in gangue quartz from the Toyoha Mine (abstract). *Abst. Joint Meet. Soc. Mining Geol. Mineral Soc. Japan, and Japan. Assoc. Mineral. Petrol. Econ. Geol.*, 26 (in Japanese).
- Metal Mining Agency of Japan (1991) Report on development of gas geochemical exploration methods during the fiscal year Heisei 2. Metal Mining Agency of Japan, Tokyo, 160p. (in Japanese).
- Metal Mining Agency of Japan (1993) Report on detailed geological survey in the Jozankei area during the fiscal year Heisei 4. Metal Mining Agency of Japan, Tokyo, 142p. (in Japanese).
- Ministry of International Trade and Industry (1999) Report of Regional Geological Structure Survey in South Hokkaido Area during the Fiscal Year Heisei 10. Ministry of International Trade and Industry, 145p. (in Japanese).
- Miyajima, T., Hakari, N. and Kita, M. (1971) Some considerations on geologic structure and mechanism of fracturing at the Toyoha mine. *Mining Geol.*, 21, 22-35 (in Japanese with English abstract).
- NEDO (1988) Report on Geothermal Development Promotion Survey, No. 12 Toyoha area: Tokyo, New Energy Development Organization, 1156p. (in Japanese).
- Ohminato, T. and Takakura, S. (1999) Seismic survey around Mt. Muine. Report of Regional Geological Structure Survey during the Fiscal Year Heisei 10: Southern Hokkaido Area. Ministry of International Trade and Industry, 125-145 (in Japanese).
- Ohta, E. (1989) Occurrence and chemistry of indium-containing minerals from the Toyoha Mine, Hokkaido, Japan. *Mining Geol.*, 39, 355-372.
- Ohta, E. (1991) Polymetallic mineralization at the Toyoha Mine, Hokkaido, Japan. *Mining Geol.*, 41, 279-295.
- Ohta, E. (1992) Silver mineralization at the Toyoha Mine, Hokkaido, Japan. *Mining Geol.*, 42, 19-32.
- Ohta, E. (1995) Common features and genesis of tin-polymetallic veins. *Resource Geol. Spec. Issue*, 18, 187-195.
- Ohta, E. and Marumo, K. (1985) Occurrence of apatite and associated gangue minerals in the Toyoha deposits, west Hokkaido, Japan. *Proc. Japan Acad.*, 61, Ser. B, 99-102.
- Ono, S. and Sato, J. (1994) Ore minerals and fluid inclusions from the veins in the northwestern part of the Toyoha Pb-Zn-Ag mining district, Hokkaido, Japan. *Resource Geol.* 44, 369-379.
- Richards, J.P. (2003) Tectono-magmatic precursors for porphyry Cu-(Mo-Au) deposit formation. *Econ. Geol.*, 98, 1515-1533.
- Rye, R.O. (1993) The evolution of magmatic fluids in the epithermal environment: the stable isotope perspective. *Econ. Geol.*, 88, 733-753.
- Rye, R.O., Bethke, P.M., and Wasserman, M.D. (1992) The Stable isotope geochemistry of acid sulfate alteration. *Econ. Geol.*, 87, 225-262.
- Sakai, H., and Ueda, H. (1984) Sulfur isotopic values of volcanic gases, in Ossako, J., ed., *Fundamental Research for Predicting Volcanic Eruption through Observation of Volcanic Gases*. Ministry of Education, Japan, No. A-59-4, 127-135 (in Japanese).

- Sanga, T., Kanbara, H., Shoji, T. and Takeyama, T. (1992) Characteristic feature of the late stage mineralization and its vein system at the Toyoha polymetallic vein deposits, Hokkaido, Japan. *Mining Geol.*, 42, 85-100 (in Japanese with English abstract).
- Sawai, O. (1984) Wall rock alteration around the Motoyama deposits, Toyoha mine, Hokkaido, Japan. *Mining Geol.*, 34, 173-186 (in Japanese with English abstract).
- Sawai, O., Okada, T. and Itaya, T. (1989) K-Ar ages of sericite in hydrothermally altered rocks around the Toyoha deposits, Hokkaido, Japan. *Mining Geol.*, 39, 191-204.
- Schwarz-Schampera, U. and Herzig, P.M. (2002) *Indium: Geology, Mineralogy, and Economics*. Springer-Verlag, Heidelberg, 257p.
- Shimizu, T. and Aoki, M. (2001a) Fluid inclusion and oxygen isotope studies of hydrothermal quartz from Yunosawa Stream and Nagatozawa Stream near the Toyoha Ag-Pb-Zn deposit, Hokkaido. *Shigen-Chishitsu*, 51, 133-144 (in Japanese with English abstract).
- Shimizu, T. and Aoki, M. (2001b) Overprinted Cenozoic hydrothermal activities at the Toyoha Ag-Pb-Zn deposit, Japan. In Cidu, ed., *Water Rock Interaction 2001*, 757-760.
- Shinohara, H., 1994, Exsolution of immiscibility vapor and liquid phases from a crystallizing silicate melt: Implications for chlorine and metal transport: *Geochim. Cosmochim. Acta*, 58, 5215-5221.
- Sillitoe, R.H. (1973) The tops and bottoms of porphyry copper deposits. *Econ. Geol.*, 63, 799-815.
- Sillitoe, R.H. (1977) Metallic mineralization affiliated to subaerial volcanism: a review. in *Volcanic Proc. Ore Genesis*. Geol. Soc. Inst. Mining Metal., London, 99-116.
- Sillitoe, R.H. (1994) Erosion and collapse of volcanoes: Causes of telescoping in intrusion-centered ore deposits. *Geol.*, 22, 945-948.
- Sillitoe, R.H. (1995) Exploration of porphyry copper lithocaps. In Mauk, J.L. and St. George, J.D., eds., *Pacrim Congress 1995*. Austral. Inst. Mining Metal., 527-532.
- Sillitoe, R.H. and Bonham, H.F., Jr. (1984) Volcanic landforms and ore deposits. *Econ. Geol.*, 79, 1286-1298.
- Takada, A. (1994) The influence of regional stress and magmatic input on styles of monogenetic and polygenetic volcanism. *Jour. Geophys. Res.*, 99, 13563-13573.
- Takakura, S. and Matsushima, N. (2003) Magnetotelluric investigation of hydrothermal system and heat source in the Muine-Toyoha geothermal area, Japan. *Resource Geol.*, 53, 213-220.
- Tsukimura, K., Sato, K. and Ishihara, S. (1987) Regional and temporal variation in FeS content of sphalerite from Japan and its relation to granitoids series. *Bull. Geol. Surv. Japan*, 38, 227-246.
- Watanabe, Y. (1989) Tectonic control on vein-type ore deposits in Sapporo-Akaigawa district, southwestern Hokkaido. *Mining Geol.*, 39, 273-281 (in Japanese with English abstract).
- Watanabe, Y. (1990a) Pliocene to Pleistocene volcanism and related vein-type mineralization in Sapporo-Iwanai district, southwest Hokkaido, Japan. *Mining Geol.*, 40, 289-298.
- Watanabe, Y. (1990b) Pull-apart vein system of the Toyoha deposit, the most productive Ag-Pb-Zn vein-type deposit in Japan. *Mining Geol.*, 40, 269-278.
- Watanabe, Y. (1993) Late Cenozoic stress field in northern part of southwest Hokkaido based on trends of dikes and craters. *Jour. Geol. Soc. Japan*, 99, 105-116 (in Japanese with English abstract).
- Watanabe, Y. (2002) Late Cenozoic metallogeny of Southwest Hokkaido, Japan. *Resource Geol.*, 52, 191-210.
- Watanabe, Y. (2003a) Hydrothermal alteration associated with the Pliocene Muine volcano and base-metal mineralization at the Toyoha deposit, northeast Japan (abstract). *Geol. Soc. Am. Abst. Programs*, Vol. 35, No. 6, September 2003, p. 552.
- Watanabe, Y. (2003b) Style of oceanic plate subduction and deposit types. In Shikazono, N., Nakano, T. and Hayashi, K., eds., *Resource and Environmental Geology*, Soc. Resource Geol., 163-170 (in Japanese).
- Watanabe, Y. and Iwata, K. (1986) Miocene stratigraphy around Toyoha Mine, southwest Hokkaido. *Jour. Geol. Soc. Japan*, 92, 817-820 (in Japanese).
- Watanabe, Y. and Ohta, E. (1995) The relation of two-stage mineralization at the Ag-Pb-Zn Toyoha deposit, southwest Hokkaido, to subduction of the Pacific plate. *Resource Geol., Spec. Issue*, 18, 197-202.
- White, N.C., Leake, M.J., McCaughey, S.N. and Parris, B.W. (1995) Epithermal gold deposits of the southwest Pacific. *Jour. Geochem. Explor.*, 54, 87-136.
- Yajima, J. and Ohta, E. (1979) Two-stage mineralization and formation process of the Toyoha deposits, Hokkaido, Japan. *Mining Geol.*, 29, 291-306.
- Yajima, J., Ohta, E. and Kanazawa, Y. (1991) Toyohaite, $Ag_2FeSn_3S_8$, a new mineral. *Mineral. Jour.*, 15, 222-232.
- Yajima, J., Ohta, E., Kamiki, T. and Takeyama, T. (1993) Formation model and exploration of the Toyoha Mine, Hokkaido, Japan. *Resource Geol., Spec. Issue*, 15, 451-458.



Vapor from the underground tunnel of the Toyoha deposit